

56840
pg4

NASA Technical Memorandum 100761

The Pioneer Venus Orbiter: 11 Years of Data

A Laboratory for Atmospheres Seminar Talk

W. T. Kasprzak

MAY 1990

ORIGINAL CONTAINS
COLOR ILLUSTRATIONS

(NASA-TM-100761) THE PIONEER VENUS ORBITER:
11 YEARS OF DATA. A LABORATORY FOR
ATMOSPHERES SEMINAR TALK (NASA) 82 p

N90-23273

CSCS 22A

Unclass

G3/88

0280465



NASA Technical Memorandum 100761

**The Pioneer Venus Orbiter:
11 Years of Data**

A Laboratory for Atmospheres Seminar Talk

W. T. Kasprzak
Goddard Space Flight Center
Greenbelt, Maryland

NASA

National Aeronautics and
Space Administration

Goddard Space Flight Center
Greenbelt, MD

1990

**ORIGINAL CONTAINS
COLOR ILLUSTRATIONS**

PREFACE

The contents of this document were originally presented as a Laboratory for Atmospheres seminar talk entitled "TEN YEARS OF VENUS DATA" on January 23, 1990.

CONTENTS

1. INTRODUCTION.....	1
2. GEOLOGY.....	17
3. ATMOSPHERE.....	27
4. IONOSPHERE/SOLAR WIND INTERACTION.....	58
5. SOLAR ACTIVITY EFFECTS.....	64
6. SUMMARY.....	77
7. REFERENCES.....	78

1. INTRODUCTION

"Pioneer 12 takes a licking but craft keeps a ticking"
(Associated Press, Dec. 6, 1988, D. M. Hunten)

The ancient astronomers knew of Venus. For example, the Mayans of central Mexico did not recognize Venus as a planet. They called it the evening star when seen in the western sky after sunset and the morning star when seen in the eastern sky before sunrise. The Mayans, however, knew the synodic period was 583.9 days. The Greeks first recognized the morning and evening star as a single object calling it Cytherea after the island sacred to Aphrodite (the goddess of love). The Romans called it Venus. Venus is the brightest object in the night sky after the moon. Its astronomical symbol is the hand mirror symbolizing its reflected brilliance. Modern data on Venus is shown in Table 1.1.

On December 4, 1978 a satellite was inserted into orbit around Venus in order to determine the salient features of the planet, its atmosphere/ionosphere, and interaction with the solar wind (ref. 4). The 10th anniversary of the Pioneer Venus Orbiter was celebrated at Ames Research Center with a symposium describing the main contributions of the Orbiter to the general understanding of Venus (ref. 1). The Orbiter has operated successfully the past 11 years gathering remote and in situ data over most of the solar cycle, and will continue operation until reentry into the atmosphere in 1992. Although Venus and Earth are often called twin planets, they are only superficially similar. Possessing no obvious evidence of plate tectonics, lacking water and an intrinsic magnetic field, and having a hot dense carbon dioxide atmosphere with sulfuric acid clouds makes Venus a unique object of study by the Orbiter's instruments.

Table 1.1. Comparison of Earth and Venus

	VENUS	EARTH	
Distance from sun	0.7	1	au
Orbital period	224.7	365.25	days
Orbit eccentricity	0.0068	0.0167	
Inclination of axis	177.4	23.4	deg
Rotation period	-243	+1	days
Relative mass	0.8	1	
radius	0.95	1	
density	0.96	1	
gravity	0.91	1	
magnetic moment	$<10^{-5}$	1	
Atmosphere			
Surface pressure	92	1	atm
Surface temperature	735	288	K
Composition	96.5% CO ₂	78% N ₂	
	3.5% N ₂	21% O ₂	
		1% A	
Clouds-composition	H ₂ SO ₄	H ₂ O	
-cover	100%	40%	
-superrotation	4	?	days
Albedo	0.8	0.3	

The quotation at the beginning of the introduction refers to the fate of the Orbiter. Since Venus is closer to the Sun than the Earth, the satellite is subject to more heating than it would at earth. The lack of an intrinsic magnetic field does not protect the satellite from the effects of solar flares. As of this date the Orbiter infrared spectrometer has failed and the magnetometer has partially failed; the solar panel power output is gradually diminishing with time; and the hydrazine fuel used for orbit maneuvers is almost gone. In 1992 the satellite will reenter the atmosphere and burnup.

The mission began as a study at Goddard Space Flight Center (ref. 2a). It soon evolved into a single orbiter and a bus carrying 4 lower atmosphere probes with project management at Ames Research Center. The mission was to be low cost (Table 1.2) (ref. 1f) with the same basic spacecraft design being used for both the orbiter and bus (the beginning of the "universal bus" concept). The Orbiter has produced quite a few data bits. Much of that data have been analyzed and reported in the literature (ref. 3).

The goals of the lower atmosphere probes and the orbiter are summarized in Table 1.3. Prior to 1962, the first spacecraft visit to Venus, quite a bit was known about the planet and there was considerable speculation about what lay underneath the obscuring clouds (Table 1.4) (ref. 281). Today, after many spacecraft visits and remote Earth observations considerably more is known. Venus has a hot, dense carbon dioxide atmosphere with high altitude sulfuric acid clouds. There are no oceans on Venus and it has been at least 4 billion years since there may have been enough water to have formed one. The lack of an intrinsic magnetic field has two implications: a) the solar wind interacts directly with the ionosphere rather than a magnetic field as in the

Table 1.2. Some Interesting Statistics About the Orbiter (Ref. 1f)

INTERESTING STATISTICS

Initial project cost	\$ 80 M
[with probes	\$ 163 M]
Science/operation cost, 10 years	\$ 45 M
Orbiter total cost, 10 years	\$ 125 M
No. of data bits returned	> 10
No. of publications	> 1000
No. of participants	> 160

13

Table 1.3. Goals of the Pioneer Venus Mission

GOALS

MULTIPROBE

- 1) Nature and composition of clouds (particle and mass analyzers)
- 2) Composition and structure of atmosphere (temperature, pressure, acceleration and mass measurements)
- 3) General atmospheric circulation (separated probes)

ORBITER

- 1) Global mapping of atmosphere by remote sensing (UV, IR, visible, radio wave, γ -ray, radio occultation)
- 2) In-situ measurements of neutral atmosphere, ionosphere, solar wind interaction region
- 3) Radar mapping of surface (93% mapped)

Table 1.4. Venus Before the First Spacecraft Visit and Now (Ref. 28i)

FACTS KNOWN ABOUT VENUS PRIOR TO 1962 (FIRST SPACECRAFT VISIT):

- 1) Rich CO₂ atmosphere
- 2) Opaque clouds obscure surface
- 3) Substantial flux at radio wavelengths
- 4) Lower atmosphere hot and dense
- 5) Surface smooth compared to Earth's

SPECULATION ABOUT VENUS:

- 1) Moist, swampy, teeming with life OR
- 2) Warm with carbonic acid ocean (i.e. selzer water) OR
- 3) Cool, Earth-like, surface water, dense ionosphere OR
- 4) Warm, massive clouds of water, continual rain with lightning OR
- 5) Cold at pole with 10-km icecaps, hot at equator with water above boiling point OR
- 6) Hot, dusty, dry, windy, global desert OR
- 7) Very hot, cloudy, molten lead and zinc puddles at equator, seas of bromine, butyric acid and phenol at poles

NOW:

- 1) Mainly CO₂ atmosphere (96.5% CO₂, 3.5% N₂); surface pressure 92 atmospheres; sulfuric acid clouds (50 to 70 km)
- 2) Virtually no water (100ppm in atmosphere; no oceans)
- 3) Rocky surface at very high temperature (735 Kelvin)
- 4) Ionosphere comparable to Earth's, no intrinsic magnetic field
- 5) Plateaus and mountains on Venus as high or higher than on Earth but lowlands only one-fifth the greatest depth of those on Earth

case of the Earth (ref. 7); b) there are no radiation belts although Venus does possess atomic oxygen aurora (refs. 5,6). The surface of Venus is generally not any higher than the Earth but it possesses no lowlands equivalent to the Earth's ocean basins.

Since 1962, 22 American and Soviet spacecraft have visited Venus as orbiters, fly-bys, lower atmosphere probes and balloons floating at the cloud tops (Table 1.5). The U.S. Magellan Mission will arrive at Venus in August, 1990. It carries a single instrument, a high resolution radar mapper. The Pioneer Venus Mission is summarized in Table 1.6 (ref. 2a). Like all projects Pioneer Venus began with a series of questions about Venus (Table 1.7) and then asked what instruments, probes, and spacecraft types could help to answer those questions. Reference 1a lists the experiments, principal investigators, guest investigators and interdisciplinary scientists for the Orbiter.

The Orbiter is shown in Figure 1.1 (ref. 2). The diameter is 2.54 m, it is 1.2 m tall, weighs 582 kg with a science payload of 43 kg. The silicon solar cells are shown as a black band around the sides. The spacecraft maintains stability by spinning about an axis indicated by the telemetry antenna. There are 12 active experiments on board the spacecraft, three of which originated at Goddard Space Flight Center (Electron Temperature Probe, Ion Mass Spectrometer and Neutral Mass Spectrometer). There are three passive experiments: a) radio occultation which uses the spacecraft antenna transmissions to deduce properties of the atmosphere and ionosphere; b) atmospheric drag which determines the atmospheric density at periapsis from changes in the orbital period; and c) gravimetrics which uses orbital perturbations to deduce surface mass concentrations.

Table 1.5. U.S. and Soviet Spacecraft Missions to Venus

SPACECRAFT	LAUNCH	COMMENT
Mariner 2	27-Aug-62	Fly-by 14-Dec-62
Venera 3	16-Nov-65	Venus impact 01-Mar-66
Venera 4	12-Jun-67	Soft atmospheric entry 18-Oct-67
Mariner 5	14-Jun-67	Fly-by 19-Oct-67
Venera 5	05-Jan-69	Soft atmospheric entry 16-May-69
Venera 6	10-Jan-69	Soft atmospheric entry 17-May-69
Venera 7	17-Aug-70	Soft surface landing 15-Dec-70
Venera 8	27-Mar-72	Soft surface landing 22-Jul-72
Mariner 10	03-Nov-73	In solar orbit: Venus flu-by 05-Feb-74; Mercury fly-by 29-Mar-74, in Sep-74 and Mar-75
Venera 9	08-Jun-75	Orbiter and surface lander 22-Oct-75
Venera 10	14-Jun-75	Orbiter and surface lander 25-Oct-75
Pioneer Venus 1	20-May-78	Orbiter: 04-Dec-78
Pioneer Venus 2	08-Aug-78	Multiprobes enter atmosphere 09-Dec-78 week after arrival of orbiter
Venera 11	09-Sep-78	Fly-by; soft lander, dayside 25-Dec-78
Venera 12	14-Sep-78	Fly-by; soft lander, dayside 21-Dec-78
Venera 13	30-Oct-81	Soft lander 01-Mar-82
Venera 14	04-Nov-81	Soft lander 05-Mar-82
Venera 15	02-Jun-83	Radar mapper 10-Oct-83
Venera 16	07-Jun-83	Radar mapper 14-Oct-83
Venera Halley 1 (VEGA 1)	15-Dec-84	Balloon 11-Jun-85 Halley's comet 06-Mar-86
Venera Halley 2 (VEGA 2)	21-Dec-84	Balloon 14-Jun-85 Halley's comet 09-Mar-86
Magellan	06-May-89	Radar mapper Aug-90 arrival
Galileo	19-Oct-89	Fly-by 10-Feb-90; remote sensing

Venera spacecraft are USSR spacecraft; the remainder are USA spacecraft. The best earth to Venus launch opportunities occur about every 19 months.

Table 1.6. Pioneer Venus Mission, Its Instrument Types and Requirements (Ref. 2a)

DATE	MILESTONE
1968	National Academy of Sciences recommends mission
1974	Spacecraft and science payload selected
1975	Start instrument design
20-MAY-1978	Launch orbiter spacecraft
08-AUG-1978	Launch multi-probe spacecraft
04-DEC-1978	Orbiter encounters Venus
09-DEC-1978	Multi-probe encounters Venus
Today	Orbiter still functioning; periapsis at 2000 km
1992	Re-enter atmosphere and burn-up

INVESTIGATION TYPE	INSTRUMENT TYPES
Atmospheric composition/ structure	Mass spectrometer Ultra-violet spectrometer Gas chromatograph Accelerometers and temperature probes
Clouds	Nephelometer Cloud particle spectrometer Photopolarimeter
Thermal balance	Infrared and solar flux radiometer
Dynamics/Turbulence	Multi-probe tracking Radio occultation
Solar wind/ionosphere	Magnetometer Electric field detector Ion mass spectrometer Electron density/temperature probe Plasma analyzer(s)
Surface/interior	Radio occultation Radar mapper Orbital celestial mechanics
Astronomy	Gamma-ray burst detector

INSTRUMENT REQUIREMENTS

Low power (solar cells, batteries)
 Low weight (launch vehicle, propellant limitations)
 Small size (" " " ")
 Adaptable to a wide range of measurement conditions
 (exploring new territory)
 Operate UNATTENDED for years (no on-site repair)
 Survive Environment (temperature, radiation, vacuum)
 Survive earth launch (vibration)

Table 1.7. Questions for the Pioneer Venus Mission (Ref. 2a)

1. Cloud layers: What is their number and where are they located? Do they vary over the planet?
2. Cloud forms: Are they layered, turbulent, or merely hazes?
3. Cloud physics: Are the clouds opaque? What are the sizes of the cloud particles? How many particles are there per cubic centimeter?
4. Cloud composition: What is the chemical composition of the clouds? Is it different in the different layers?
5. Solar heating: Where is the solar radiation deposited within the atmosphere?
6. Deep circulation: What is the nature of the wind in the lower regions of the atmosphere? Is there any measurable wind close to the surface?
7. Deep driving forces: What are the horizontal differences in temperature in the deep atmosphere?
8. Driving force for the 4-day circulation: What are the horizontal temperature differences at the top layer of clouds that could cause the high winds there?
9. Loss of water: Has water been lost from Venus? If so, how?
10. Carbon dioxide stability: Why is molecular carbon dioxide stable in the upper atmosphere?
11. Surface composition: What is the composition of the crustal rocks of Venus?
12. Seismic activity: What is its level?
13. Earth tides: Do tidal effects from Earth exist at Venus, and if so, how strong are they?
14. Gravitational moments: What is the figure of the planet? What are the higher gravitational moments?
15. Extent of the 4-day circulation: How does this circulation vary with latitude on Venus and depth in the atmosphere?
16. Vertical temperature structure: Is there an isothermal region? Are there other departures from adiabaticity? What is the structure near the cloud tops?
17. Ionospheric motions: Are these motions sufficient to transport ionization from the day to the night hemisphere?
18. Turbulence: How much turbulence is there in the deep atmosphere of the planet?
19. Ion chemistry: What is the chemistry of the ionosphere?
20. Exospheric temperature: What is the temperature and does it vary over the planet?
21. Topography: What features exist on the surface of the planet? How do they relate to thermal maps?
22. Magnetic moment: Do the planet have internal magnetism?
23. Bulk atmospheric composition: What are the major gases in the Venus atmosphere? How do they vary at different altitudes?
24. Anemopause: How does the solar wind interact with the planet?

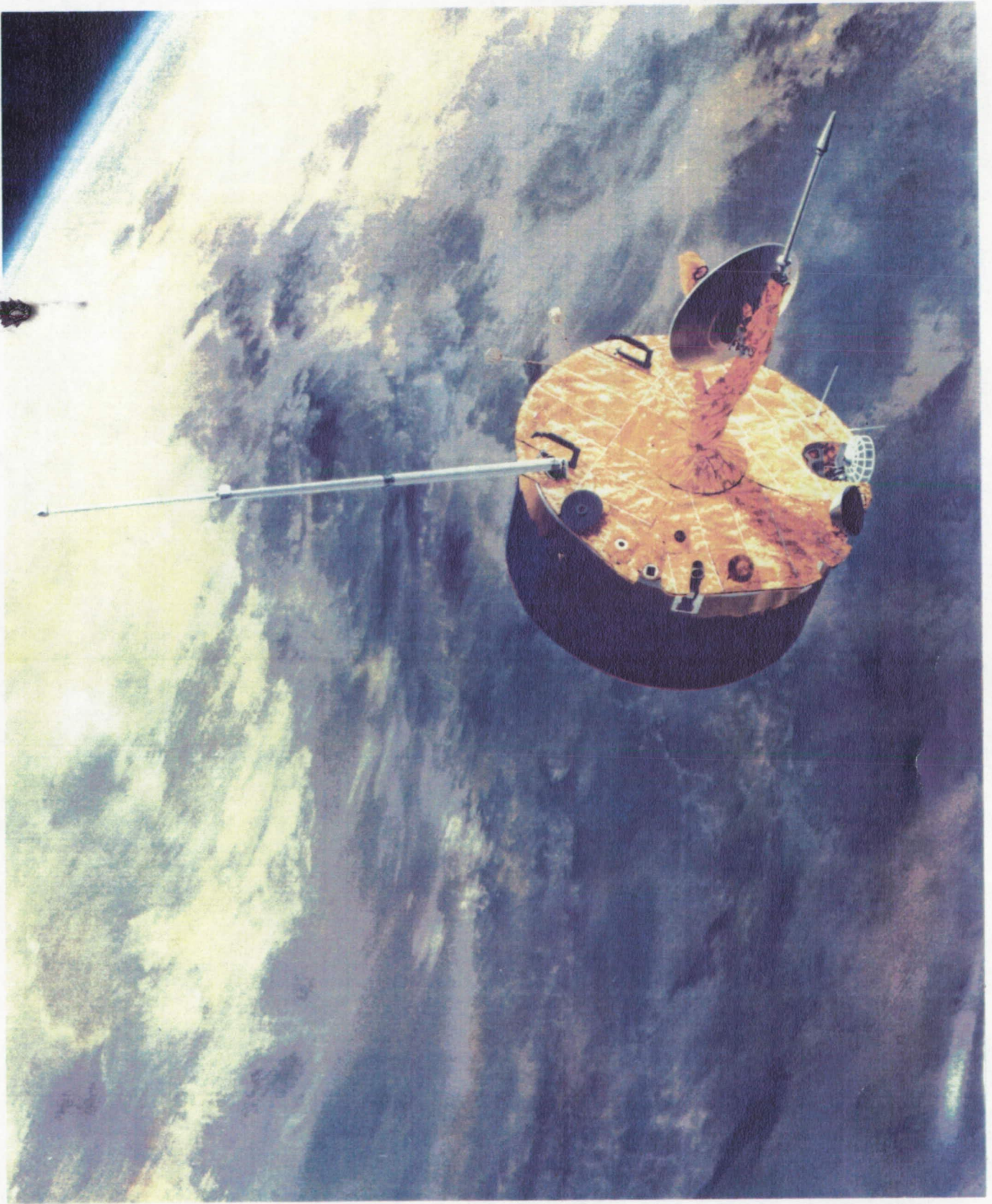


Figure 1.1. An artist's conception of the Orbiter in place around Venus (ref. 2).

Figure 1.2 (refs. 2a,2b) shows the situation at the initial encounter with Venus. The Orbiter is in place around the planet and the lower atmosphere probes, having been released from the Bus, impact on the surface at the locations shown. The Bus, carrying an ion and neutral mass spectrometer, will burn up near the morning terminator. The orbit is nearly polar with an inclination of about 15 degrees, has a nominal 24 hour period, with initial periapsis near 150 km and apoapsis near 66000 km. The position of the orbit in 1978-80, during initial encounter, and in 1992, during the final reentry phase, are shown in the bottom of figure 1.2.

The evolution of the orbit's periapsis altitude is shown in Figure 1.3 (ref. 2b). For the first 600 orbits periapsis was maintained near 150 km by propulsion. In situ measurements of the atmosphere and main ionosphere were possible during this phase. After this period periapsis was allowed to drift upward to a maximum of 2300 km due solar gravitational perturbations and is now drifting downward due to the same perturbation. In 1992 the spacecraft will reenter the atmosphere and finally burn up.

A comparison of Earth and Venus to scale is shown in Figure 1.4 (ref. 8a). The picture of Venus was taken in the ultraviolet to show the cloud structure. As can be seen in Table 1.1 Earth and Venus are very similar in radius, mass, density and gravitational acceleration. The sulfuric acid clouds rotate about the planet once every 4 days in a retrograde fashion (contrary to the direction of rotation of the Earth). This may not seem remarkable until it is realized that the planet takes 243 days to complete one rotation about its axis. The axis of Venus is almost perpendicular to its orbit plane and the orbital eccentricity is very small so that there are no seasons on Venus.

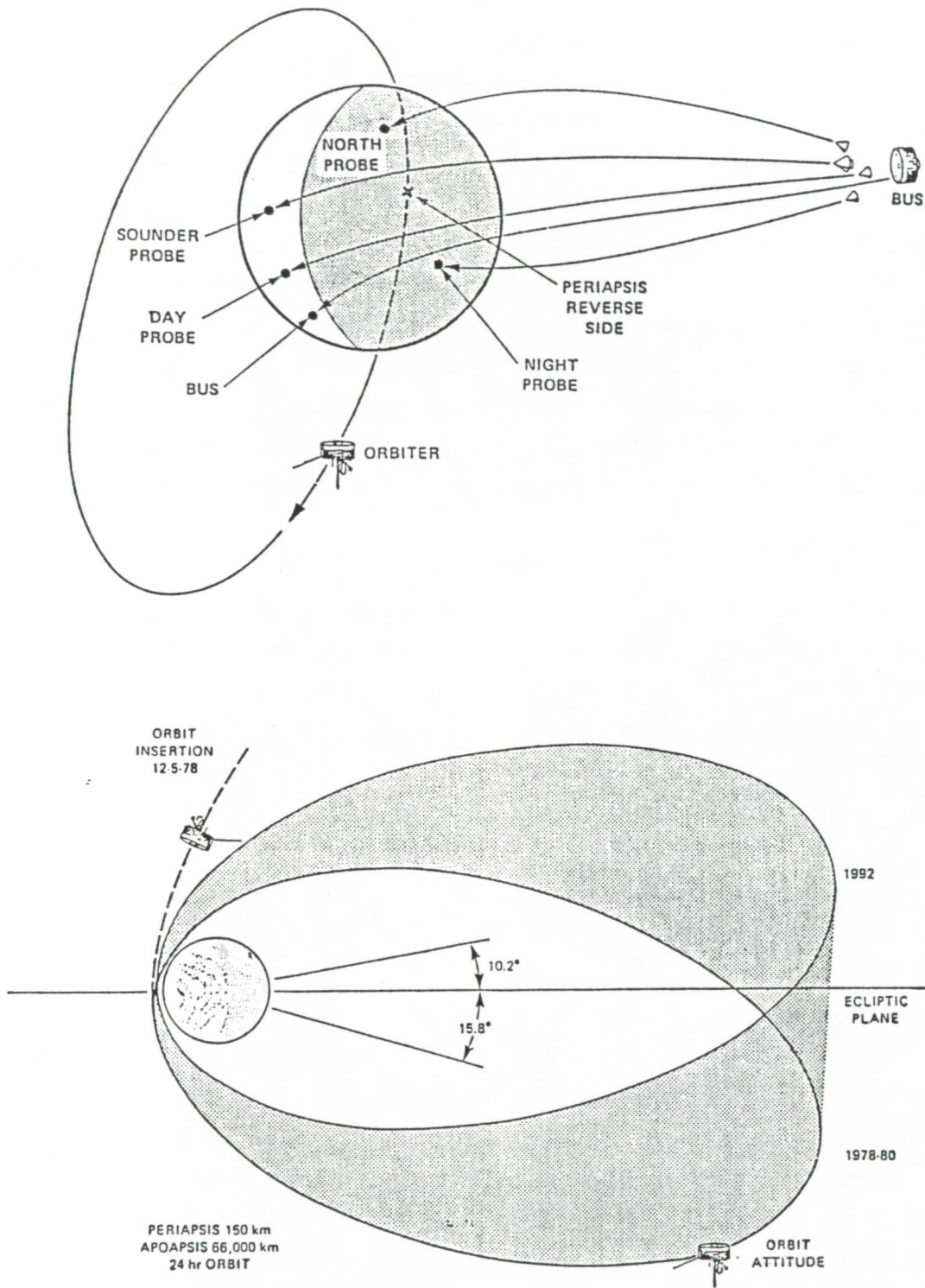


Figure 1.2. The Orbiter in position, the bus has released its probes (top) (ref. 2a). The orbit as it appeared in 1978-80 and as it will appear in 1992 (bottom) (ref. 2b).

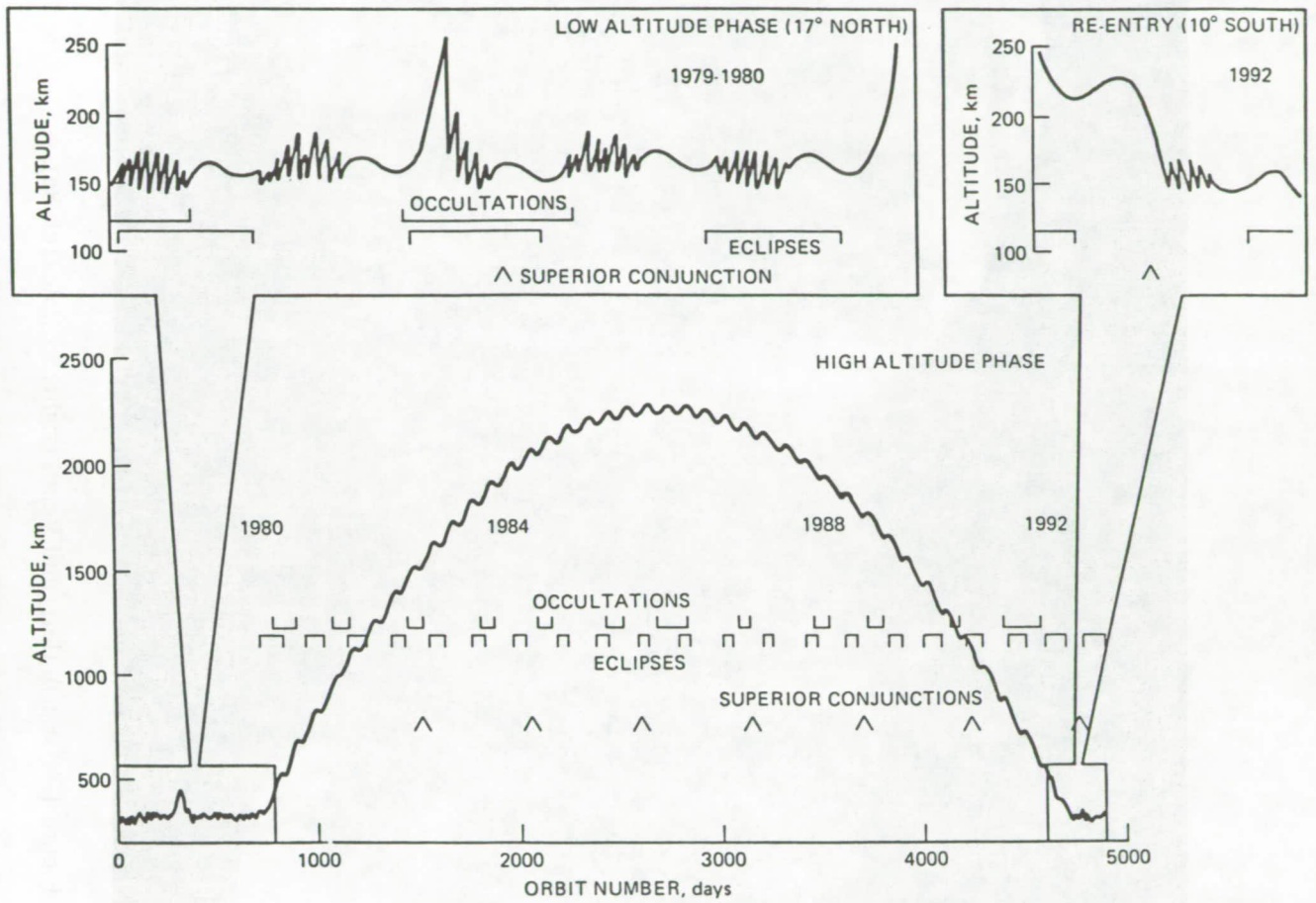


Figure 1.3. The evolution of the periapsis altitude of the orbit (ref. 2b).

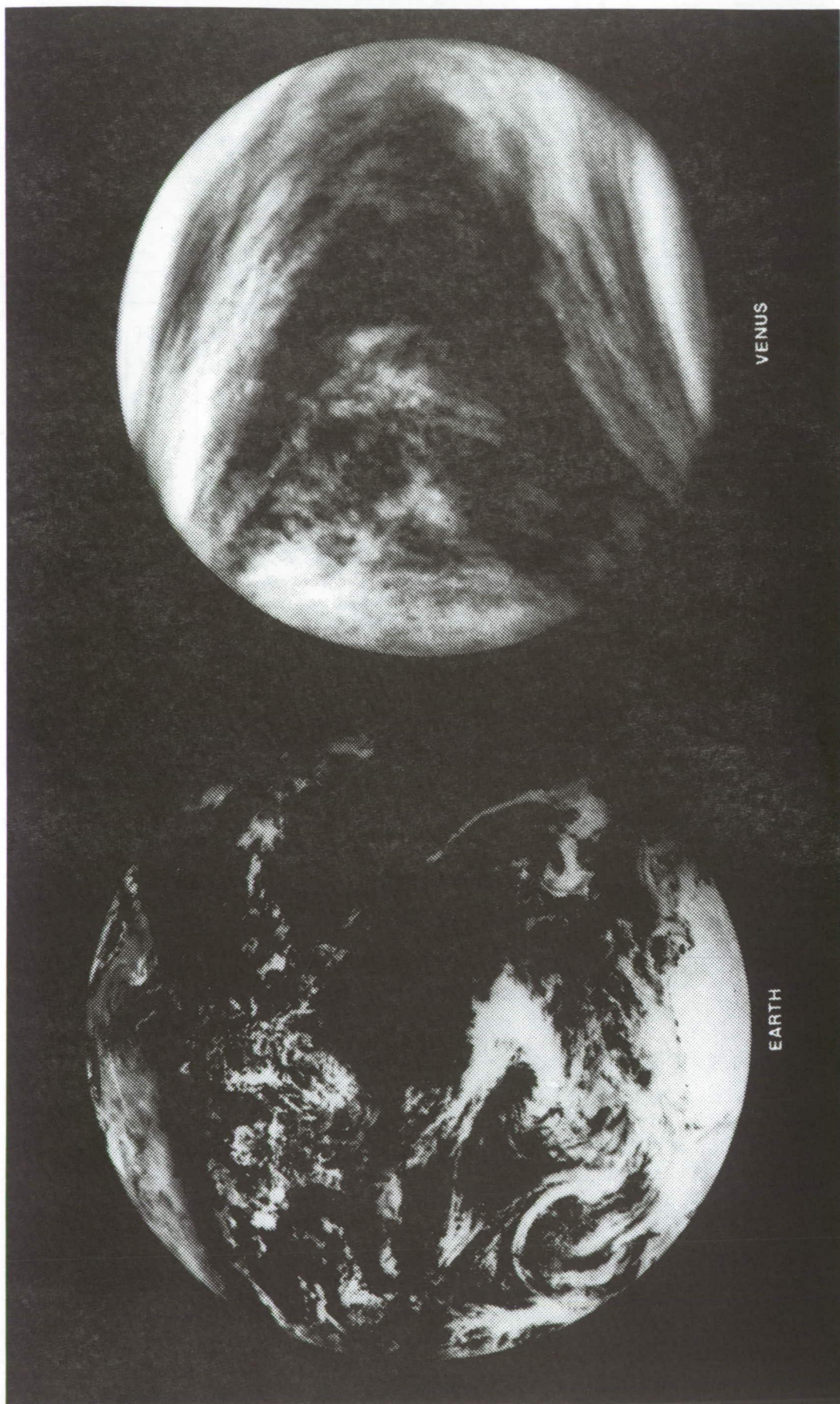


Figure 1.4. Earth (left) and Venus (right) to scale (ref. 8a).

2. GEOLOGY

The upper limit on the magnetic moment in Table 1.1 is based on magnetometer data (ref. 9). The implication is that today Venus has no active internal dynamo. The requirements for a planetary dynamo (refs. 10,11) are: a) an electrically conducting fluid such as iron which is usually present in the core of planets and has a conductivity comparable to copper at high temperatures; and b) convective motion of the fluid (for example, a helical motion along the main direction of motion has been suggested for the Earth). The energy source can be: a) radioactive decay of potassium 40; b) settling of a denser iron phase through a less dense phase; or c) the latent heat of fusion when the core freezes out. Models (ref. 11) of the Venus core suggest that it has a slightly higher core temperature and lower core pressure than the Earth and that this has prevented the core from freezing out. With not enough heat flux or planetary rotation to drive the convection, the core stratifies. No internal dynamo or external magnetic field develops.

Earth and Venus differ internally as well as externally on the surface (ref. 17). Figure 2.1 shows the hypsographic graph of Venus derived from radar measurements; Earth is also shown (ref. 12,15). The percentage of area within a one kilometer altitude interval relative to a mean surface (sea level for the Earth and 6051.4 km for Venus) is plotted as a function of the altitude. Earth has a distinctly bimodal distribution reflecting the continents (about 35% of the area centered on zero) and the ocean basins (about 65% centered around -5 km). Venus is distinctly unimodal with 60% of the surface within a half kilometer of the mean surface. The continental regions of Venus are not generally higher than those of the Earth but a large fraction of Earth's oceans are 5-6 km below sea level unlike Venus (ref. 28f).

HYPSOGRAPHIC CURVES FOR EARTH AND VENUS

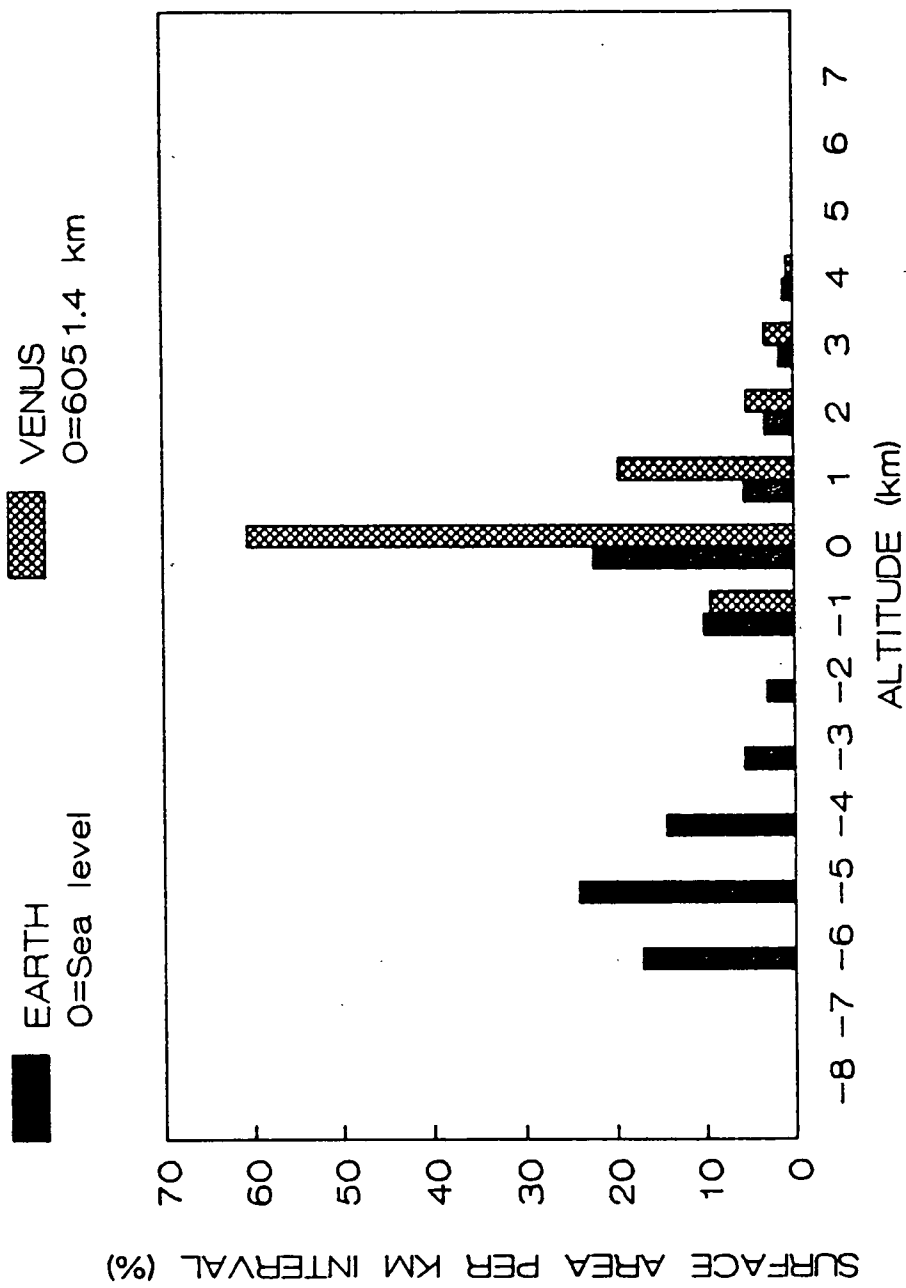


Figure 2.1. Hypsographic curve for Venus and Earth (ref. 12).

Figure 2.2 (refs. 2c,13) shows the topographic map for Venus. In the top panel, the highlands are indicated by hatched shading and represent areas higher than 2 km above the mean surface. Ishtar Terra is about the size of Australia. Maxwell Montes is the highest feature on Venus (11 km), taller than Mount Everest, and looks like an ancient volcano. Aphrodite Terra is the size of Africa and possesses gigantic rift valleys comparable to those seen on Mars. Currently there is a controversy as to whether Aphrodite represents a spreading center like the mid-Atlantic ridge on Earth (refs. 1b,14). Beta Regio consists of 2 gigantic, cone shaped, shield volcanoes similar to those seen in Hawaii. It has been suggested that this feature is being supported by similar convective processes. The dotted areas in the top panel, the lowlands, represent surfaces that are below the mean surface level. The white areas are the rolling plains between the highlands and lowlands. Some features look like meteor impact craters and crater size counts imply the surface is between 500 million years to 1 billion years old (refs. 12). The existence of the highlands seems to imply that there is little water in the rocks of Venus, at least compared to Earth standards, since water rich crustal rocks at the high temperature of Venus would tend to flow and the highlands would flatten out (ref. 18). The gravitational field closely matches the continental topography (ref. 16). Apparently significant relaxation has occurred similar to the old mountain ranges on Earth (ref. 1b). The radar topography and surface roughness are very suggestive of basaltic lava flows of the effusive or "oozing" type rather than the more explosive type (ref. 25).

Altimeter data for Venus derived from the radar mapper is shown in Figure 2.3 (refs. 8b,19); white is the highest altitude area and blue the lowest. Earth has been processed

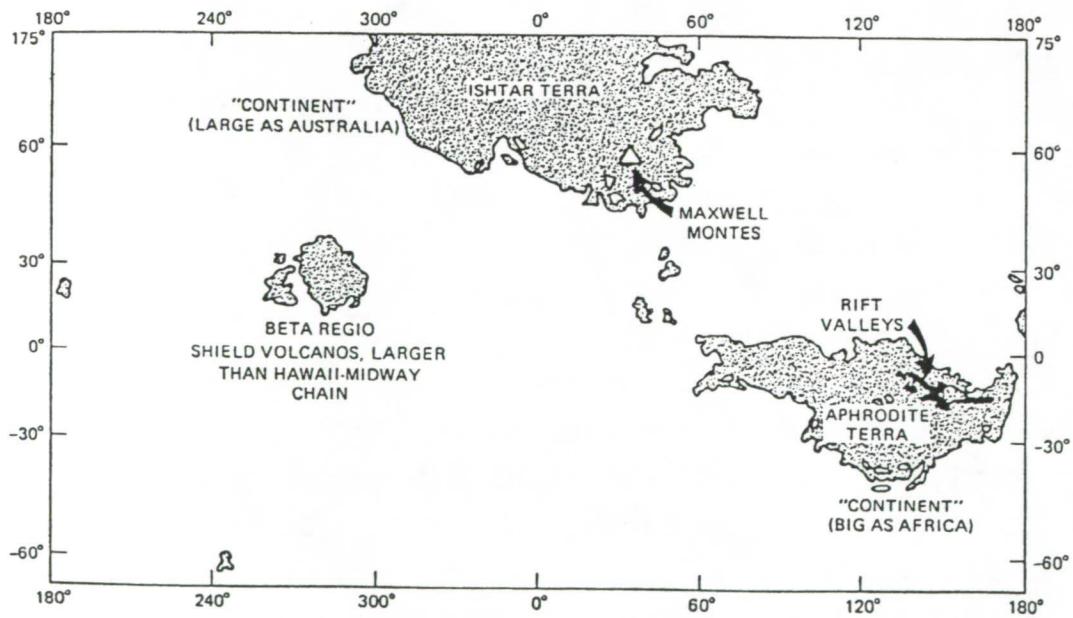
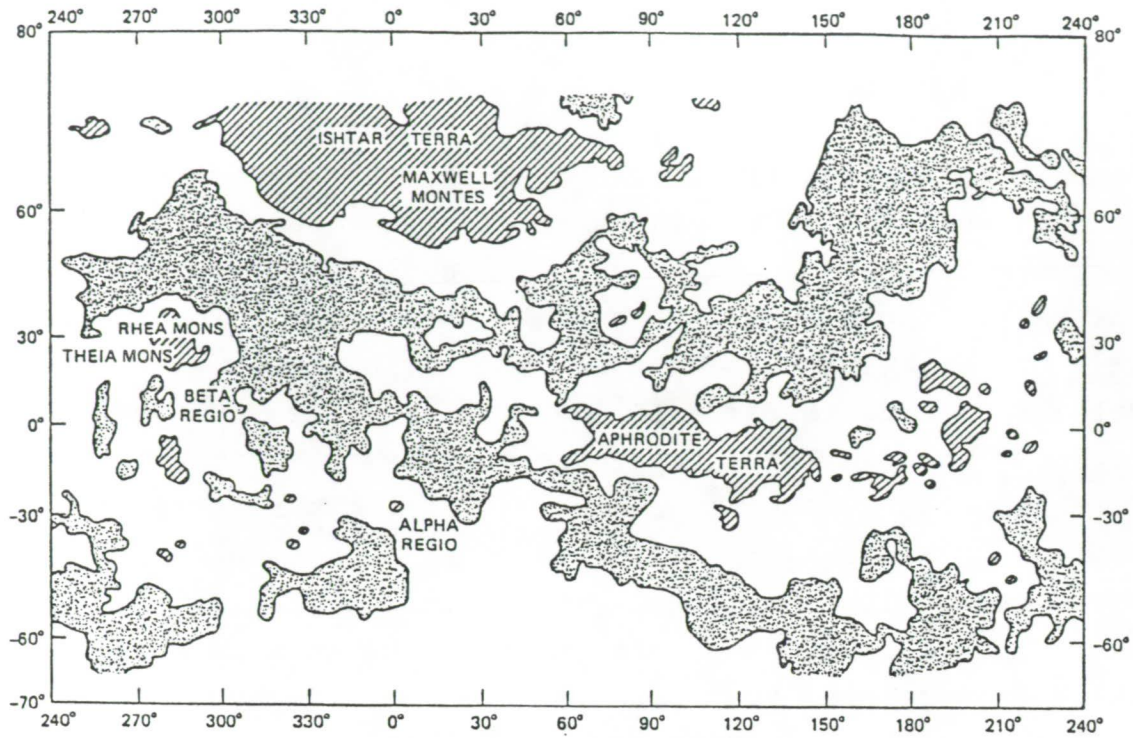


Figure 2.2. Topographic map of Venus (top) (ref. 2c). "Continental" regions in the bottom panel (bottom) (ref. 2c).

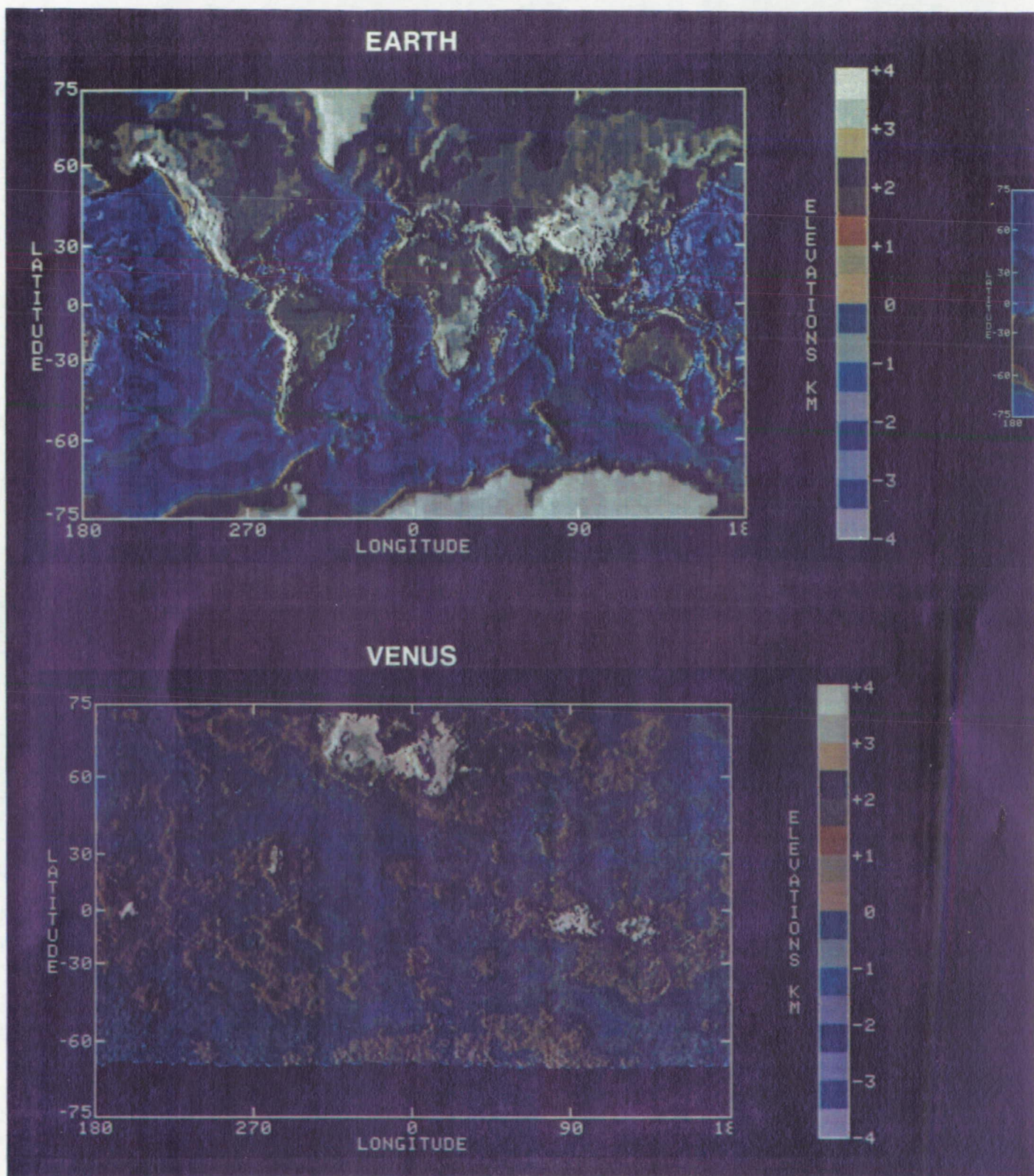


Figure 2.3. Radar views of Venus (bottom) and Earth (top) processed to the same resolution as that available from the Orbiter radar mapper (ref. 8b).

to the same spatial resolution as is available from the radar mapper on Venus. Venus has no tell-tale ridges or rifts. There are no characteristic jigsaw patterns around the continents. There is a lack of mid-ocean ridges and subduction trenches where the sea floor slides beneath the continental plates. Plate tectonics, so dominant on earth, seems to play minor role, if any, on Venus. Models of the surface suggest the high surface temperature has led to the development of a thick basaltic crust that cannot be subducted (ref. 28f). The heat release appears to be through conduction, similar to the "hot spot" volcanoes on the Earth like the Hawaiian chain which are not associated with plate boundaries (refs. 16,21,42).

Pictures of the surface of Venus have been taken by Soviet Venera spacecraft landing near Beta Regio (refs. 24,25). X-ray fluorescence measurements confirm a basaltic composition of the surface (i.e. silicate minerals high in iron and magnesium) (refs. 15,16,22,23,28g). Figure 2.4 (ref. 26) shows two surface pictures of Venus. The curvature in the picture is a result of the method used in taking the picture. The top panel shows the surface as it appears in natural light. The yellow color is due to incident light on Venus which has virtually all of the blue region of the spectrum scattered out by the atmosphere and clouds. The lower panel shows the "true" color of the surface as it would appear in white light with the atmosphere component removed. The surface of Mars is rust colored due to iron oxides; Venus might be expected to be similar in color. At 500 C dark red ferric minerals are red only in the infrared, black in the visible. The reflectance spectrum is consistent with basaltic minerals having a ferric component. The iron oxides could act as a sink for the oxygen associated with the assumed high abundance of water in the early days of Venus. In this scenario water is photodissociated into hydrogen

(which escapes from the planet) and oxygen which combines with the surface minerals. The iron oxides are also important in the geologic sulfur cycle.



Brown University

Figure 2.4. Pictures of the surface of Venus in natural light (top) and as it would appear in white light with the atmosphere component removed (bottom) (ref. 26).

3. ATMOSPHERE

Figure 3.1 shows the temperature distribution and nomenclature for the atmosphere of Earth (ref. 27a) and Venus (ref. 28a). For Earth the boundary between the stratosphere and the mesosphere has a temperature maximum due to ultraviolet absorption by ozone. On Venus there is no detectable temperature maximum in this region and ozone is below detectable limits (Table 3.1) (ref. 27b,28b). There is no stratosphere on Venus. From bottom to top: the troposphere extends from the ground to the bottom of the cloud layer (about 50 km); the mesosphere extends from there to the point where the temperature increases; the thermosphere (or "hot" sphere) extends to the exobase; and the exosphere from the exobase upward. In the exosphere the density scale height is comparable to or greater than the mean free path and particles can execute ballistic trajectories from one part of the planet to another (ref. 27e). The dotted line is the cold nightside thermosphere and exosphere (exospheric temperature near 100 K), colder than the underlying mesosphere, called the cryosphere (or "cold" sphere). The orbiter in situ measurements occur above 140 km in the exosphere. The mesosphere is where most of the ultraviolet absorption and chemical activity takes place. The chlorine chemistry keeps the ozone and molecular oxygen below detectable limits (ref. 1c). It is also responsible for maintaining the stability of carbon dioxide in the thermosphere and exosphere (ref. 27c). Chlorine also plays a role in the destruction of ozone in the Antarctic ozone hole (ref. 1c) on Earth. The planetary cold trap (ref. 27a) for Earth is near the tropopause at 15 km, 195 C. Below this level the water vapor content of the troposphere is variable but of the order of several percent. Above this level, in the stratosphere, it is about 5 ppm. The tropopause acts as a laboratory cold trap condensing out water and preventing it from going above the ozone layer

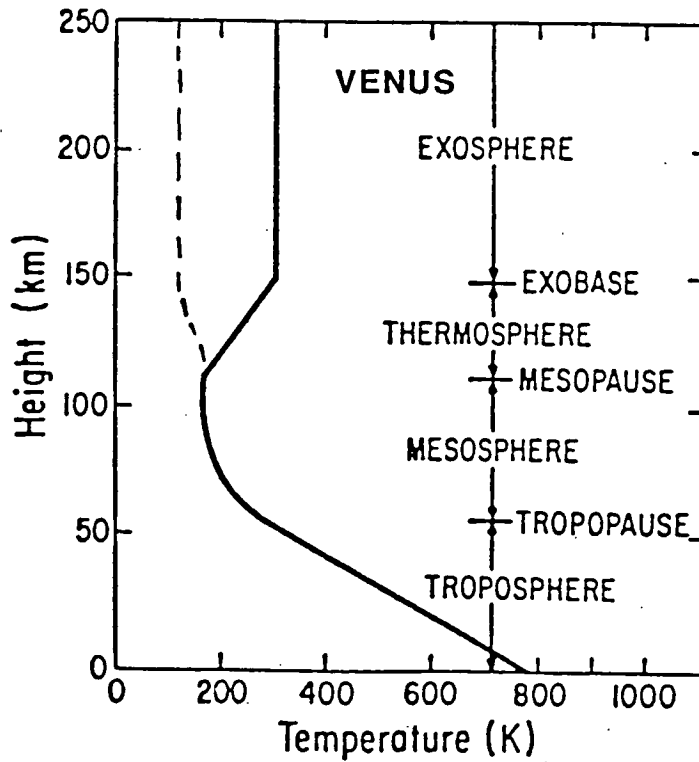
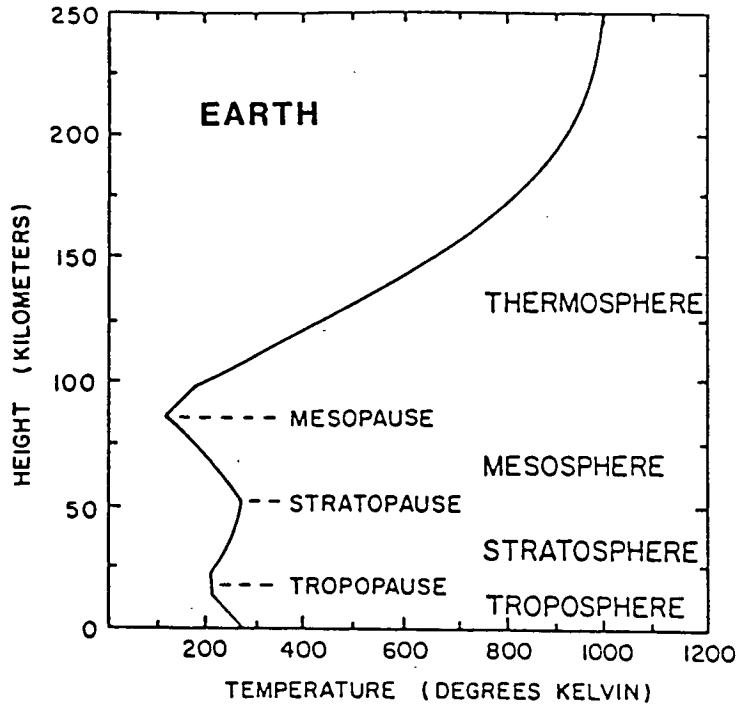


Figure 3.1. Temperature structure of Earth (top) (ref. 27a) and Venus (bottom) (ref. 28a).

Table 3.1. Fractional Composition of the Venus Atmosphere (Refs. 27b, 28b)

FRACTIONAL COMPOSITION OF ATMOSPHERES

	EARTH	VENUS
SURFACE PRESSURE	1	92 atm
CLOUD TOP PRESSURE	---	0.2 atm
GASES		
CO ₂	0.03 % (a) 96.5 %	
N ₂	78 %	3.5 %
O ₂	21 %	< 0.1 ppm
H ₂ O	0-2 % (b) < 100 ppm	
A	0.9 %	70 ppm
H ₂	0.5 ppm	?
He	5 ppm	12 ppm
CO	0.2 ppm	50 ppm
NO	0.0005 ppm	--
O ₃	0.4 ppm	--
HCl	---	0.6 ppm
HF	---	0.005 ppm
Ne	18.2 ppm	7 ppm
Kr	1.14 ppm	< 1 ppm
Xe	0.087 ppm	< 0.1 ppm
D/H	0.00015	0.02

(a) about 60 bars equivalent in crust

(b) about 270 bars equivalent in oceans

where it could be readily dissociated by ultraviolet radiation. On Venus the planetary cold trap is located near 100 km and the highly convective atmosphere can transport water to altitudes where it can be easily photodissociated.

Another interesting difference between Earth and Venus is the high deuterium to hydrogen ratio (Table 3.1) (ref. 28b), about a factor of 100 more on Venus than on Earth. The measurements are based on data from the lower atmosphere mass spectrometer (ref. 32) and inferred from the Orbiter ion mass spectrometer (refs. 33,34). This ratio has been used to constrain models of the water vapor escape from Venus (refs. 29-31). Currently, Venus has about 10 to 100 cm equivalent liquid water depth in its atmosphere (ref. 1c). The carbon dioxide and molecular nitrogen inventories per gram of planet material for Venus is about one-third less than that of the Earth (ref. 31) implying that a similar outgasing has occurred, especially of water. There are many ways for gases to escape from an atmosphere ranging from thermal (Jeans) escape to hydrodynamic flow in which species like HH and HD are equally removed. Models (refs. 29,30) for water escape differ on whether the water exists on the surface for extended period of time (moist greenhouse) or immediately evaporates into the atmosphere (runaway greenhouse). In the moist greenhouse model there is an earthlike ocean near 100 C and an atmosphere of about 1 bar of carbon dioxide. The water vapor mixing increases to 20%, the atmosphere warms up and hydrodynamic escape of hydrogen ensues entraining heavier species like oxygen in the flow. The process works with the lower solar constant expected in the early days of Venus. The outflow continues until pressure reaches 0.4 bar, after several hundred million years, leaving hydrogen to escape by normal mass discriminating processes (ref. 71) resulting in an D/H ratio of about 2%.

The radiation budget of Venus is shown in Figure 3.2. About 80% of the incident light is scattered back to space by Mie scattering of the cloud particles and Rayleigh scattering of the atmosphere (ref. 28c). About 10% is absorbed above 64 km, 10% below 64 km, and 2.5% at the surface (ref. 28d,e). With no atmosphere the surface temperature of Venus would be about 325 K; with a carbon dioxide atmosphere the temperature increases by about 410 K due to the greenhouse effect. For the Earth a more modest 35 K results primarily from the greenhouse effect of water vapor (ref. 29). The greenhouse effect is due to the relative transparency of the atmosphere in the visible, where the sun's energy is a maximum, and high opacity in the infrared where the Planck curve of the planet's surface is a maximum (ref. 27a). Models of the Venus atmosphere indicate that the current high temperature is due to the carbon dioxide greenhouse effect (ref. 1c,35). On the left of Figure 3.2 is the radiation budget for Venus and Earth (ref. 36a). The average thermal emission is indicated in solid lines and the incident energy by a dashed line at the top of the atmosphere for Venus and Earth. Venus is about 60% less than Earth in both categories. The expectation is that Venus being closer to the sun should receive about a factor of 2 more radiation than the Earth but due to the high albedo it receives less energy than the Earth. There is a net heating at the equator and cooling at the poles implying that dynamics is responsible for transporting the heat from the equator to the pole.

The transport from equator to the pole is hypothesized to be due to several single Hadley cells lying above one another (Figure 3.3, top) (refs. 28c,41). The main cell for Venus is at the cloud levels where most of the energy is absorbed. In the case of the Earth the major energy absorption is close to or at the surface in the tropics. Also on Earth, due to the Coriolis acceleration, there is one cell

$$\frac{\text{INCIDENT VENUS}}{\text{INCIDENT EARTH}} = 1.9$$

INCIDENT	100%
REFLECTED	80%
ABSORBED	
ABOVE 64km	10%
BELOW 64km	10%
AT SURFACE	2.5%

GREENHOUSE EFFECT
EARTH $\Delta T = 35K$
(H_2O, CO_2)

VENUS $\Delta T = 410K$
(CO_2)

(CHANGE IN SURFACE
TEMPERATURE)

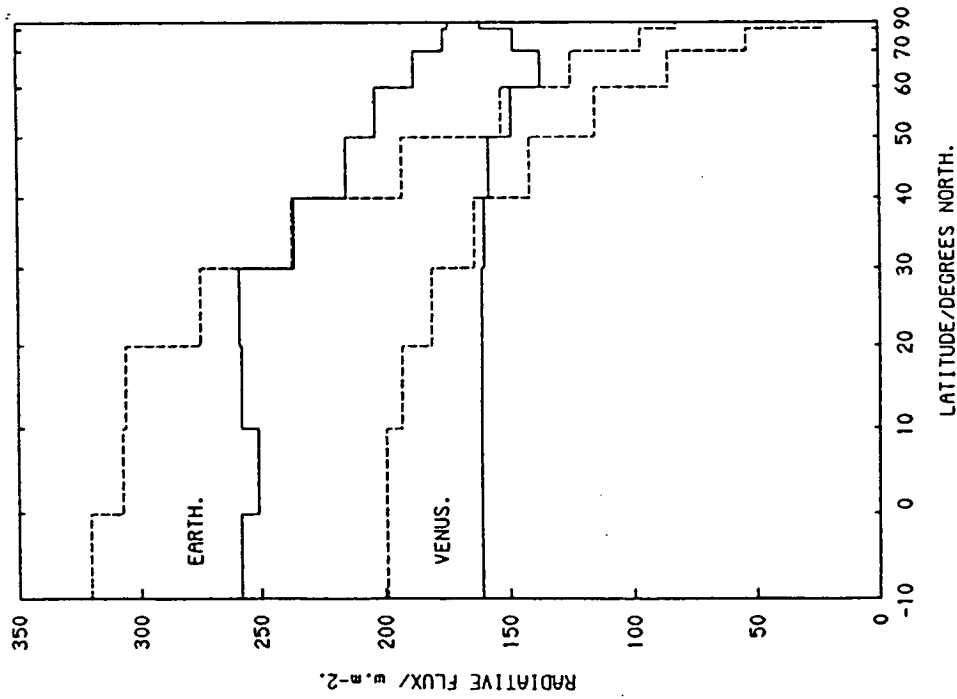


Figure 3.2. Radiation budget of Venus (ref. 36a).

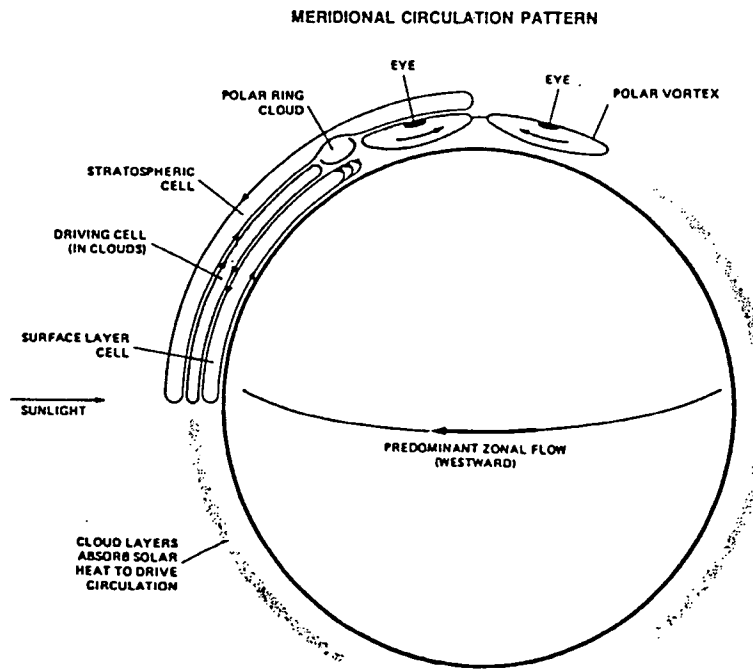
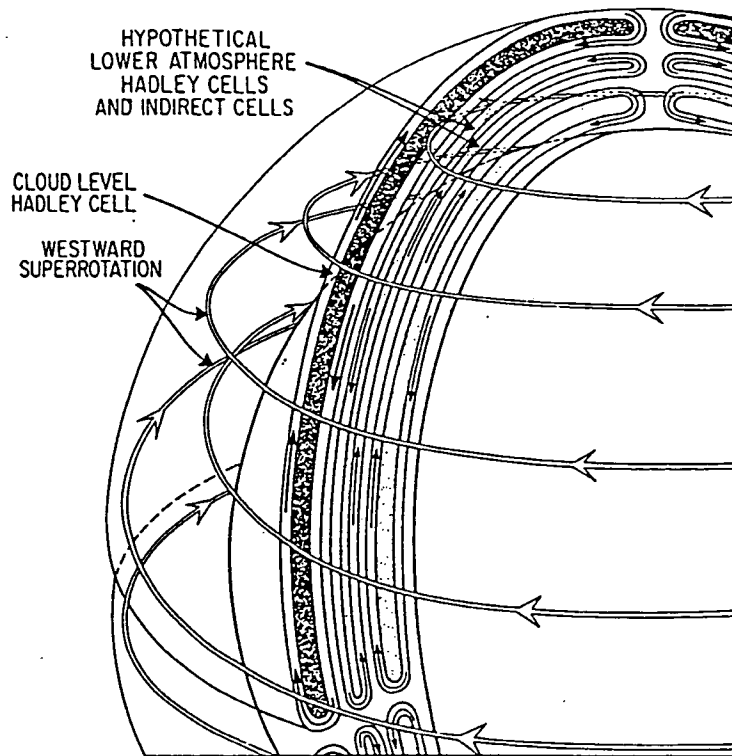


Figure 3.3. Hypothesized circulation of the lower atmosphere (top) (ref. 28c). Polar “hot” spots (bottom) (ref. 38).

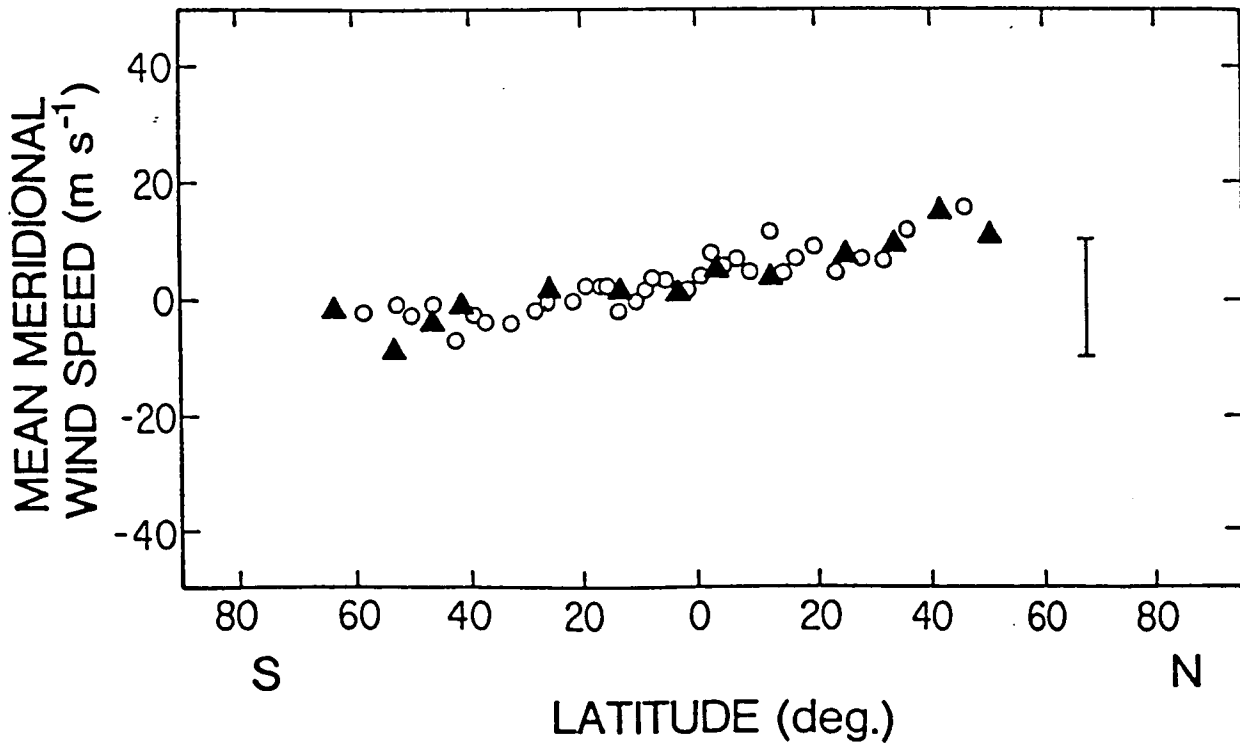
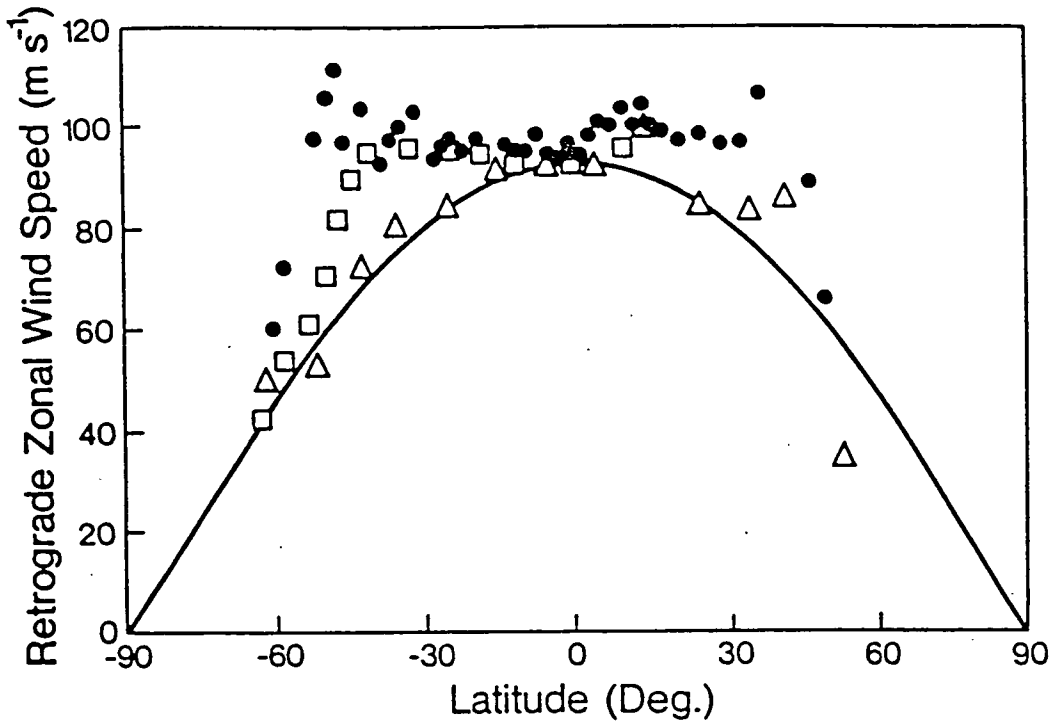


Figure 3.4. Measurements of retrograde zonal flow (top) and the meridional flow (bottom) from cloud photopolarimeter measurements (ref. 28c).

from the equator to mid-latitudes and a complicated set of baroclinic eddies from there to the pole (refs. 27d,37). The main circulation is the retrograde zonal flow observed at the cloud tops by the cloud photopolarimeter (ref. 28c) shown in Figure 3.4 (top). The triangles are Orbiter measurements, the solid circles and squares are Mariner observations. The solid curve is a solid body rotation of 92 m/s or about 4.8 day period at the equator. The meridional flow is less than 10 m/s (Figure 3.4, bottom). At the cloud tops there is a quasi-cyclostrophic balance between the meridional pressure gradient and the centrifugal force of the zonal flow. Near the north pole (Figure 3.3, bottom) there are two infrared "hot spots" rotating around each other with a period of about 2.9 days (ref. 38). The polar collar is cooler than surrounding regions. The large scale circulation keeps the equator to pole temperatures rather uniform. The wind speeds near the surface are less than 10 to 20 cm/s and probably reach a maximum of 120 m/s above 65 km. Balloon measurements show that there are vertical winds of up to 12 km/hr at 54 km, the middle of the cloud layers and considerable turbulence (ref. 39).

Another interesting phenomenon at the cloud tops is the sulfur dioxide concentration determined by the ultraviolet spectrometer from an absorption feature around 2700 Angstroms (Figure 3.5) (ref. 1d), plotted as a function of year. The measurements occur at about 40 mb or 69 km and show a decrease from the time of orbit insertion until the middle of 1988. Measurements of the sulfur dioxide below the tops and sulfuric acid vapor also show a decrease during this time period (ref. 40). The decrease in sulfur dioxide has been interpreted as evidence of volcanic activity (ref. 42) either by: a) direct injection of sulfur dioxide to 70 km, the cloud tops; or b) by gravity wave resulting from an explosive eruption mixing the nearly 500 times greater sulfur

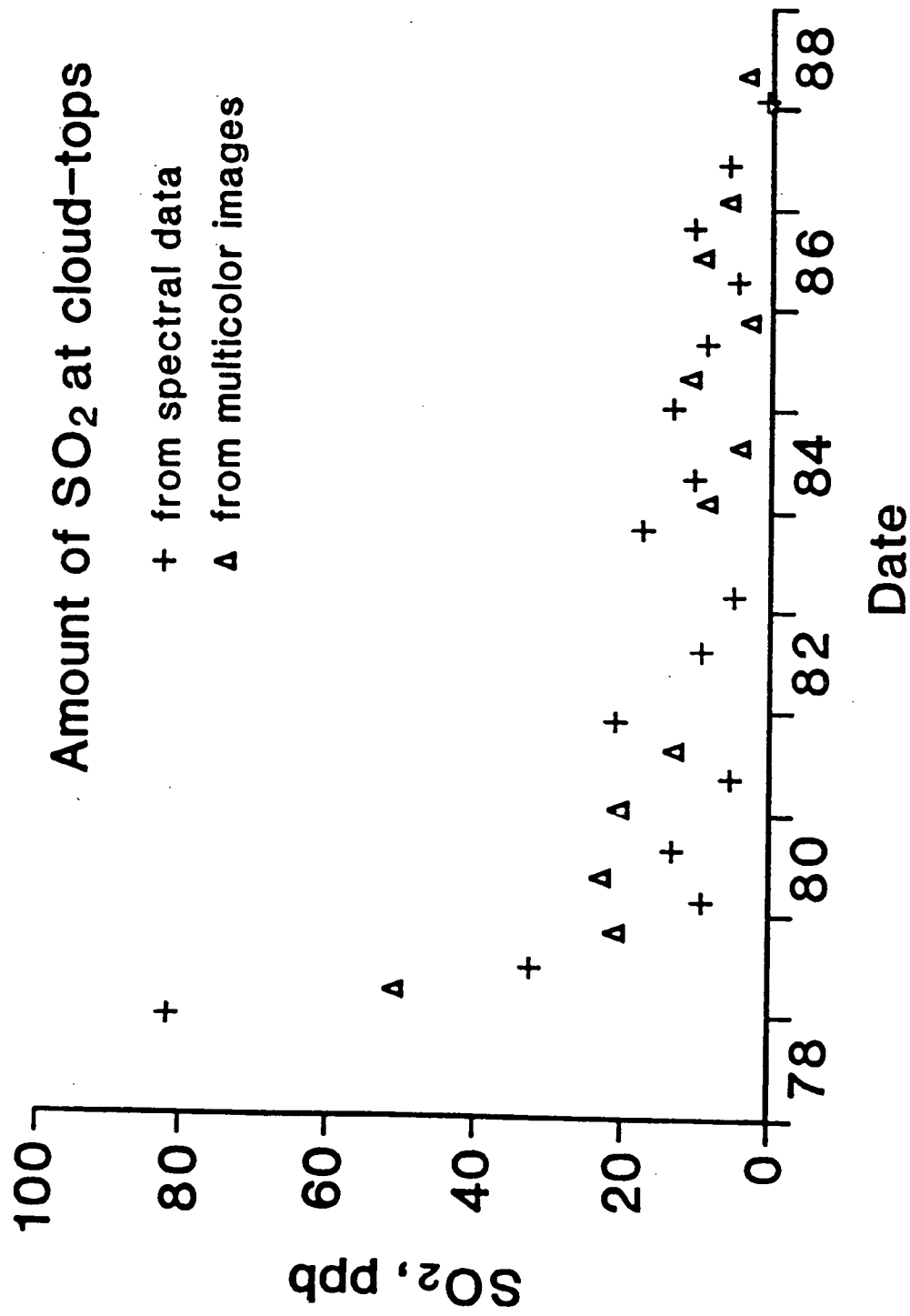


Figure 3.5. Sulfur dioxide measurements at the cloud tops (ref. 1d).

dioxide content below the clouds into the cloud tops, where the measurement occurs. The decline results from the gradual dissipation of the enhancement. However, it appears that effusive eruptions are more characteristic of the surface of Venus. The lack of water may prevent explosive eruptions (ref. 1d) such as occur on the Earth near plate boundaries.

The sulfur cycle of Venus is shown in Figure 3.6 (ref. 42,28b). The "squiggles" represent light photons. The clouds, consisting of more than 75% sulfuric acid droplets, range from 50 to 70 km altitude. There is about one water molecule per sulfuric acid molecule. There are three sulfur cycles. The fast cycle, occupying about 1 year, involves sulfuric acid, sulfur dioxide and sulfur trioxide together with atomic oxygen and carbon monoxide derived from the photodissociation of carbon dioxide. Oxidation to sulfuric acid is aided by hydrogen and chlorine from the photodissociation of hydrogen chloride. The slow cycle, occupying about 10 years, involves carbonyl sulfide, hydrogen sulfide and allotropes of elemental sulfur. It is thought that the yellow color of Venus (Figure 3.7) (ref. 20) is due to presence of elemental sulfur. The geologic cycle, lasting perhaps 500 million years, converts sulfur dioxide to calcium sulfate and then to iron pyrite aided by iron oxide. The pyrite is thermochemically converted to hydrogen sulfide and carbonyl sulfide either under ground or in lava flows.

The temperature structure of the Venus atmosphere derived from various measurements is shown in Figure 3.8 (ref. 28h). Below 100 km the data are from lower atmosphere probes and infrared measurements. The temperature gradient below the cloud layers is slightly less than adiabatic (about 1 K/km less). There are layers around 20 and 50 km that are significantly unstable (ref. 41). The optical depth of the cloud layers is about 20 to 25 (ref. 43) and turbulence is

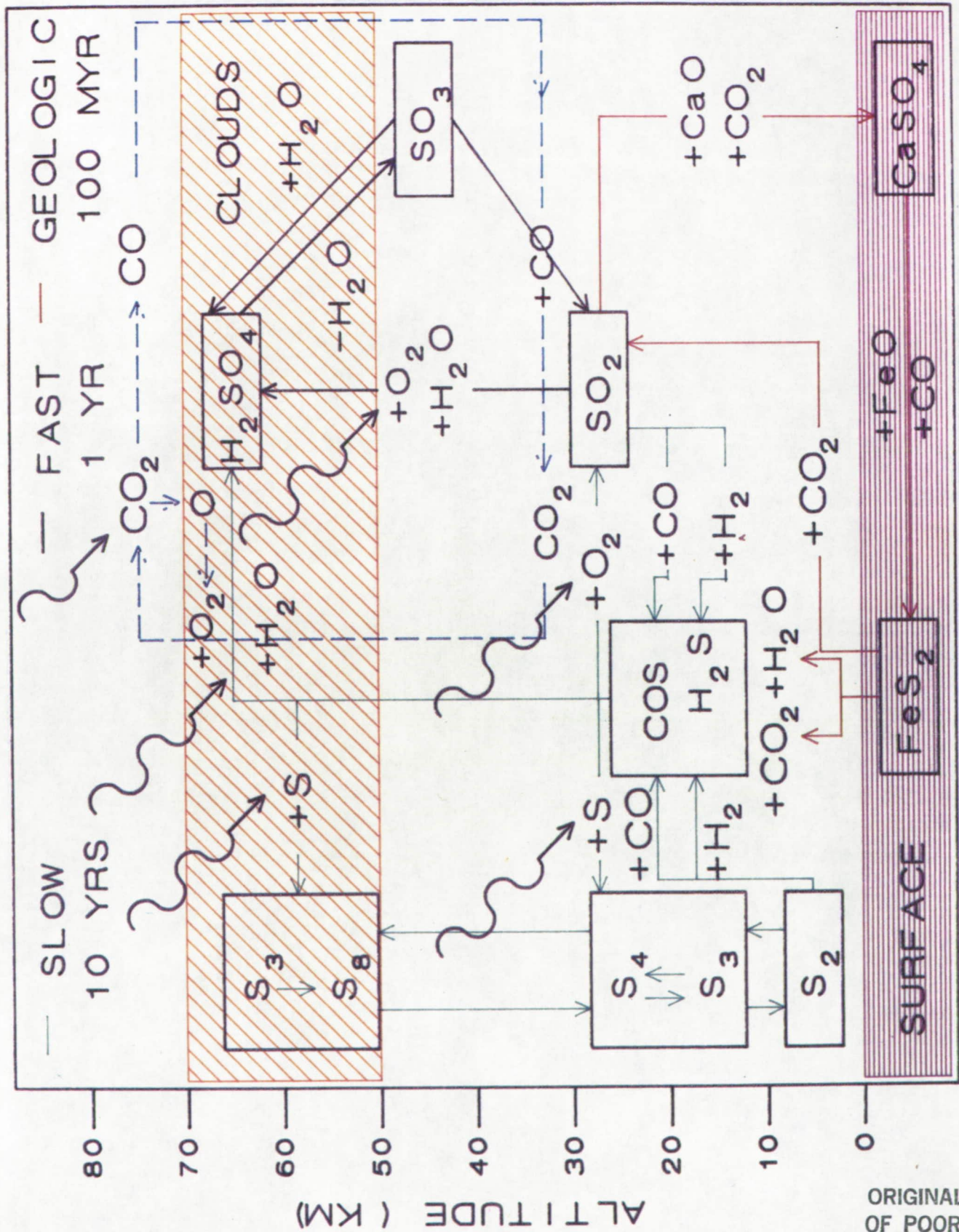
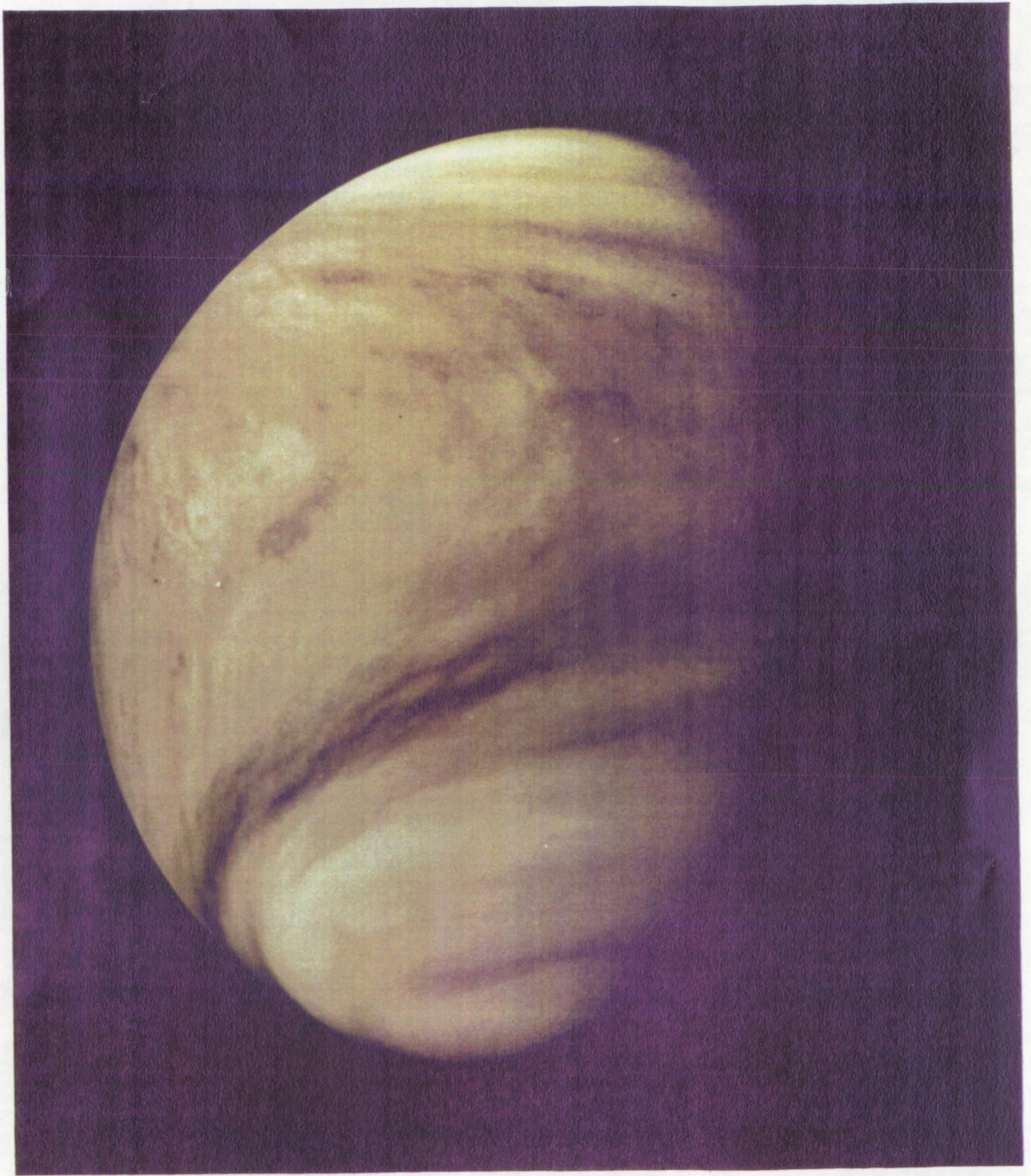


Figure 3.6. The sulfur cycle of Venus (after ref. 42).

ORIGINAL PAGE IS OF POOR QUALITY



ORIGINAL PAGE IS
OF POOR QUALITY

Figure 3.7. The color of the Venus clouds (ref. 20).

ORIGINAL PAGE
COLOR PHOTOGRAPH

PAGE 40 INTENTIONALLY BLANK

PRECEDING PAGE BLANK NOT FILMED

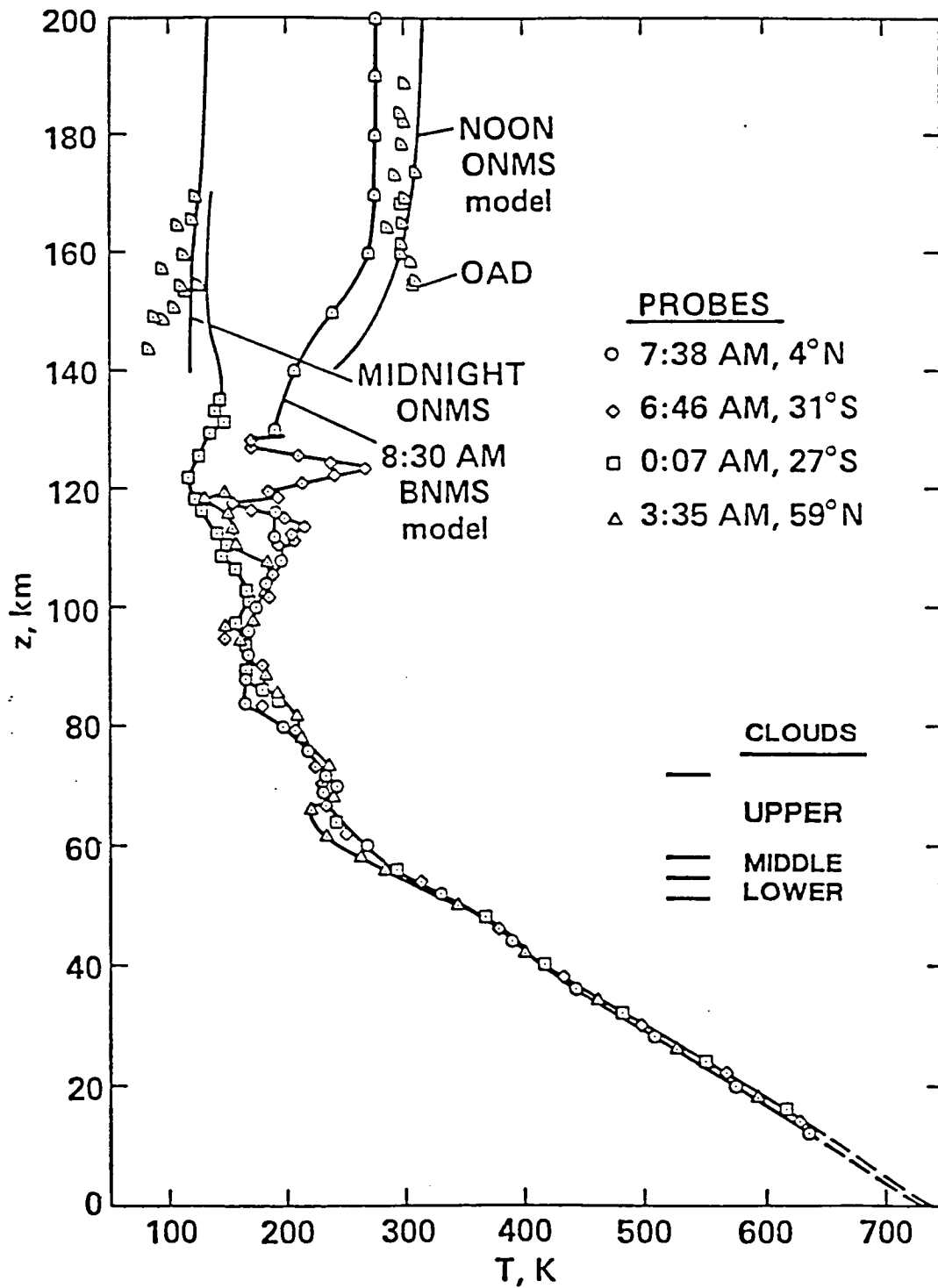


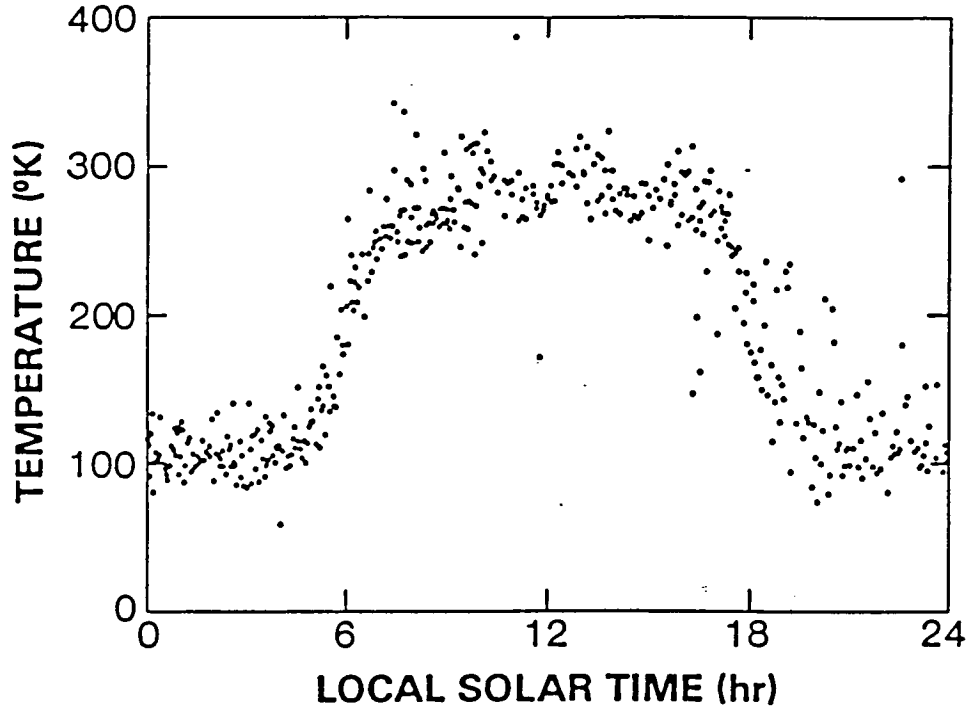
Figure 3.8. Temperature measurements of the Venus atmosphere (ref. 28h).

observed near 60 km from radio occultation measurements (ref. 44). The lower atmosphere is rather uniform in temperature horizontally, a reflection of the large thermal inertia of the atmosphere and the fact that the time scale for dynamic processes is much less than the radiative time scale (ref. 27d). On Earth the oceans show very little day to night temperature difference for the same reason. In the 100 to 140 km region there are wave-like structures in the temperature. Above 140 km temperatures from an empirical model of the neutral mass spectrometer data show a temperature of about 320 K at noon and about 130 K at midnight. Temperatures from satellite drag and the mass spectrometer on board the bus are also shown.

The region from 100 to 140 km is a transition region from a mixed atmosphere below to one in diffusion equilibrium above (ref. 27d). In a mixed atmosphere all species, in the absence of chemistry, adopt the same density scale height and have a constant mixing ratio. This is due to the fact that the time to establish diffusion equilibrium over the distance of a scale height is large compared to the time scale of dynamic processes like wind and turbulence. In diffusion equilibrium the reverse is true and each species acts independently of other species, adopting a scale height characteristic of its mass. The point where the eddy diffusion coefficient is equal to the molecular diffusion coefficient is termed the turbopause and for helium at noon it is about 114 km (ref. 45).

The effect of diffusion equilibrium on the densities measured in the exosphere is shown in the altitude profile of Figure 3.9 (bottom) (ref. 46). The scale height is inversely proportional to the species mass and proportional to the temperature. Note that atomic oxygen is dominant above 160 km, not carbon dioxide; at night helium is dominant above

DIURNAL EXOSPHERIC TEMPERATURE



DAYTIME ALTITUDE VARIATION

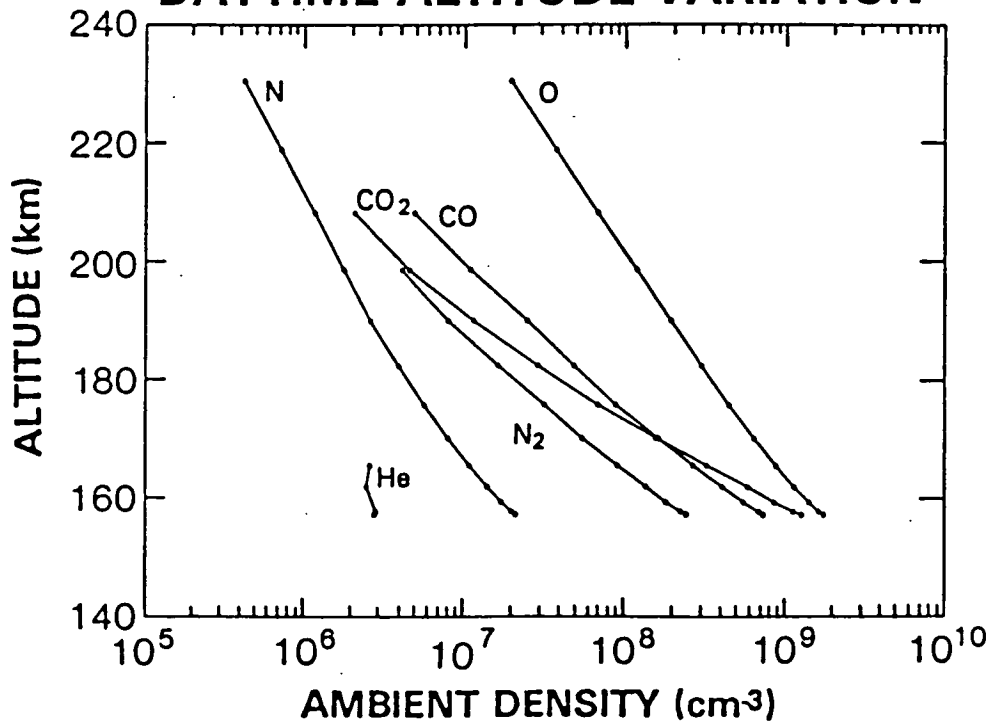


Figure 3.9. Neutral mass spectrometer exospheric temperatures derived from atomic oxygen (top) and the altitude variation of the composition at noon (bottom) (ref. 46).

about 180 km.

Exospheric temperatures derived from the scale heights of atomic oxygen are shown in the top panel of Figure 3.9 as a function of local solar time. It takes 225 days, the orbital period (Table 1.1), to cover one cycle in local solar time (ref. 281). The periodic maxima observed during the daytime are a result of the 29 day solar rotation in the euv heating of the thermosphere.

The diurnal variation of carbon dioxide and helium are shown in Figure 3.10 (ref. 28b). The data are shown at a fixed altitude of 167 km. In carbon dioxide the maximum density occurs at noon where the sub-solar heating is a maximum. There is a large day to night ratio and a steep density gradient near the terminators. The strong gradients in temperature and density at the terminators imply a strong pressure gradient and winds approaching the velocity of sound (about 200 m/s in carbon dioxide (ref. 46)). However, helium peaks near 5 am in the morning not near noon. This is due to the combined effects of wind-induced diffusion and super-rotation of the atmosphere (ref. 47). Horizontal flow in diffusion equilibrium is such that the height integrated flux is proportional to the species scale height (ref. 27a,e). Vertical flow downward through the turbopause is proportional to the mean mass scale height. The effect of wind-induced diffusion is to create a light mass gas (i.e. hydrogen and helium) bulge at midnight. Super-rotation of the atmosphere shifts the bulge to 5 am in the morning. A spectral model (ref. 47) of the Venus thermosphere found the super-rotation period to be between 4 and 8 days with a best fit period of 6 days. The direction is westward like that of the lower atmosphere and it appears that the whole atmosphere of Venus super-rotates. A recent conjecture (ref. 48) suggests that planetary atmospheres should super-rotate.

NEUTRAL THERMOSPHERE

DIURNAL DENSITY VARIATION

167 KM

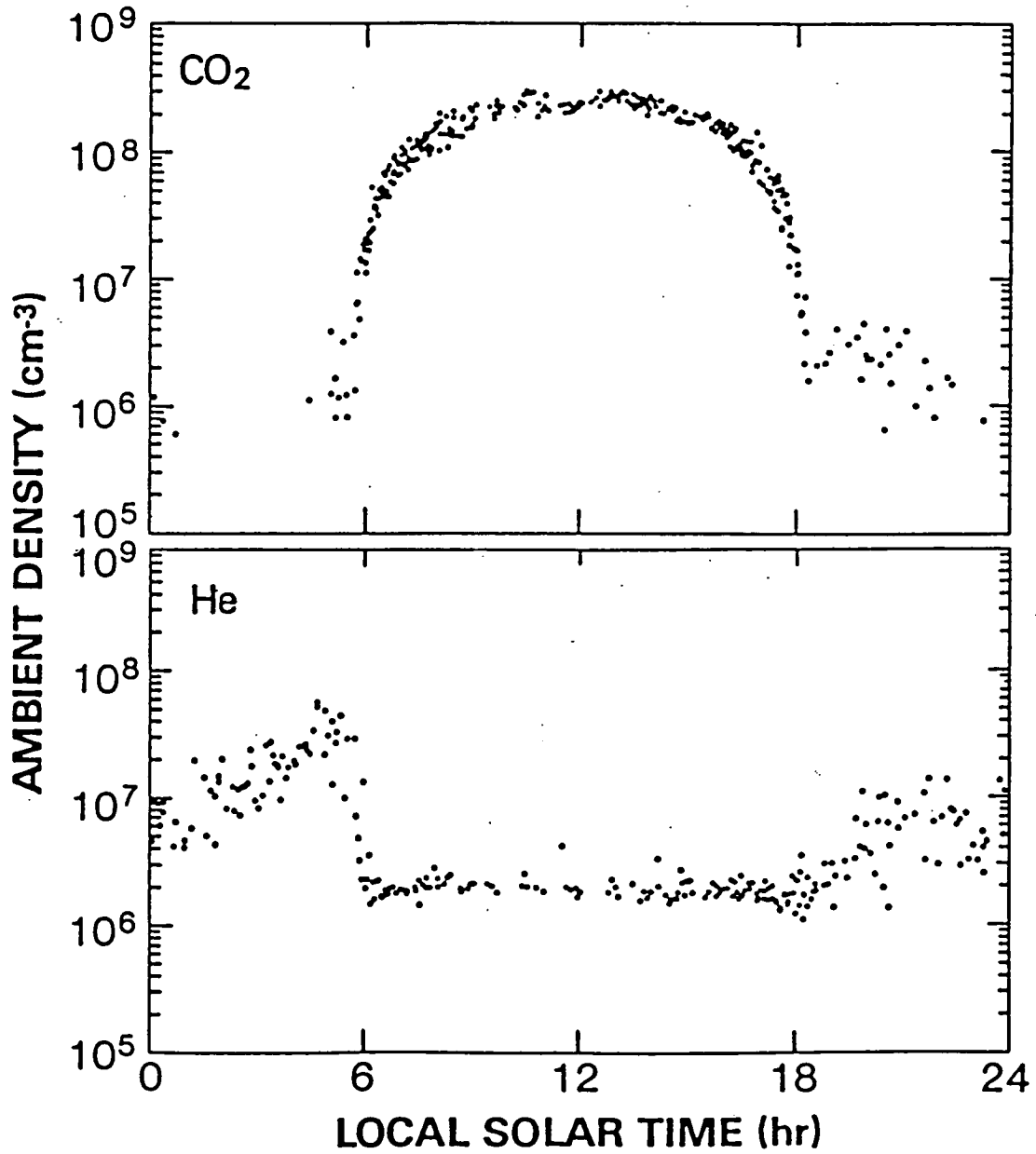


Figure 3.10. Densities from the neutral mass spectrometer for carbon dioxide (top) and helium (bottom) at a fixed altitude as a function of local solar time (ref. 28b).

A pre-dawn bulge is also seen in neutral hydrogen (Figure 3.11 ,top)) (ref. 36b). Neutral hydrogen at 165 km was derived from charge exchange equilibrium using ion mass spectrometer measurements of O⁺ and H⁺ and neutral mass spectrometer measurements of O (ref. 49). As can be seen from Figure 3.11 (bottom) the bulge in neutral hydrogen is due to the bulge in H⁺ (ref. 51). The hydrogen bulge has also been seen in the Lyman-alpha data from the ultraviolet spectrometer (ref. 50).

Figure 3.12 shows a map of the airglow due to nitric oxide, the delta (0,1) band at 2365 A, from ultraviolet spectrometer measurements (ref. 52). The horizontal axis is local solar time: midnight is at the center, 6 hours at the left and 18 hours at right. The vertical axis is latitude: the north pole is at the top and the south pole at the bottom with the equator in the center. Yellow is the maximum emission and blue the minimum emission. The maximum emission altitude is near 110 km and is due to the recombination of atomic nitrogen and atomic oxygen. These species are created on the dayside, transported at high altitude across the terminator to the nightside and subside to recombine at lower altitude. The nitric oxide glow is a tracer of the circulation and the signal maximum occurs at the local time where the vertical transport is a maximum.

The transport is displayed in a contour map of the horizontal winds from a spectral model of the thermosphere (ref. 47) at 170 km, Figure 3.13. There is an upwelling near the subsolar point on the equator and flow across the terminator with a speed near 100 m/s to a subsistence point near 3 am in the morning. The circulation probably closes around 90 km. In current models of the thermosphere (refs. 47,53) the low nightside temperature is generated by slowing

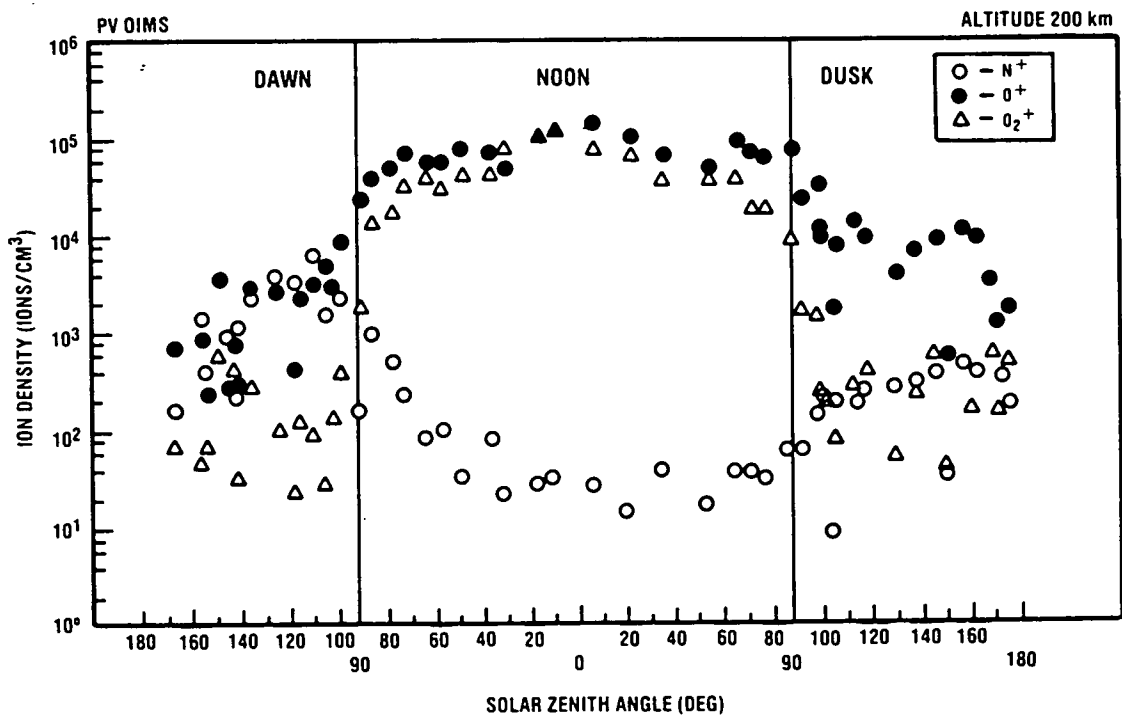
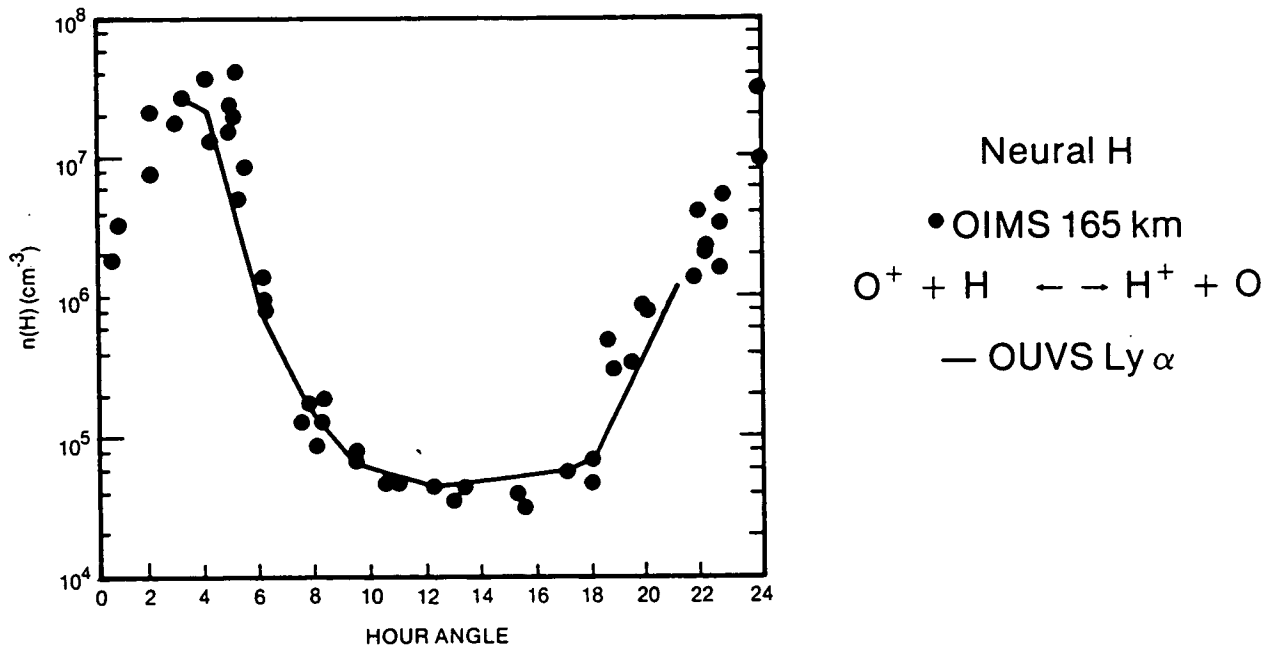


Figure 3.11. Neutral hydrogen derived from measurements of the ion and neutral mass spectrometers and from Lyman-alpha measurements (top) (ref. 50). The diurnal variation of H⁺ and O⁺ densities (bottom) (ref. 51).

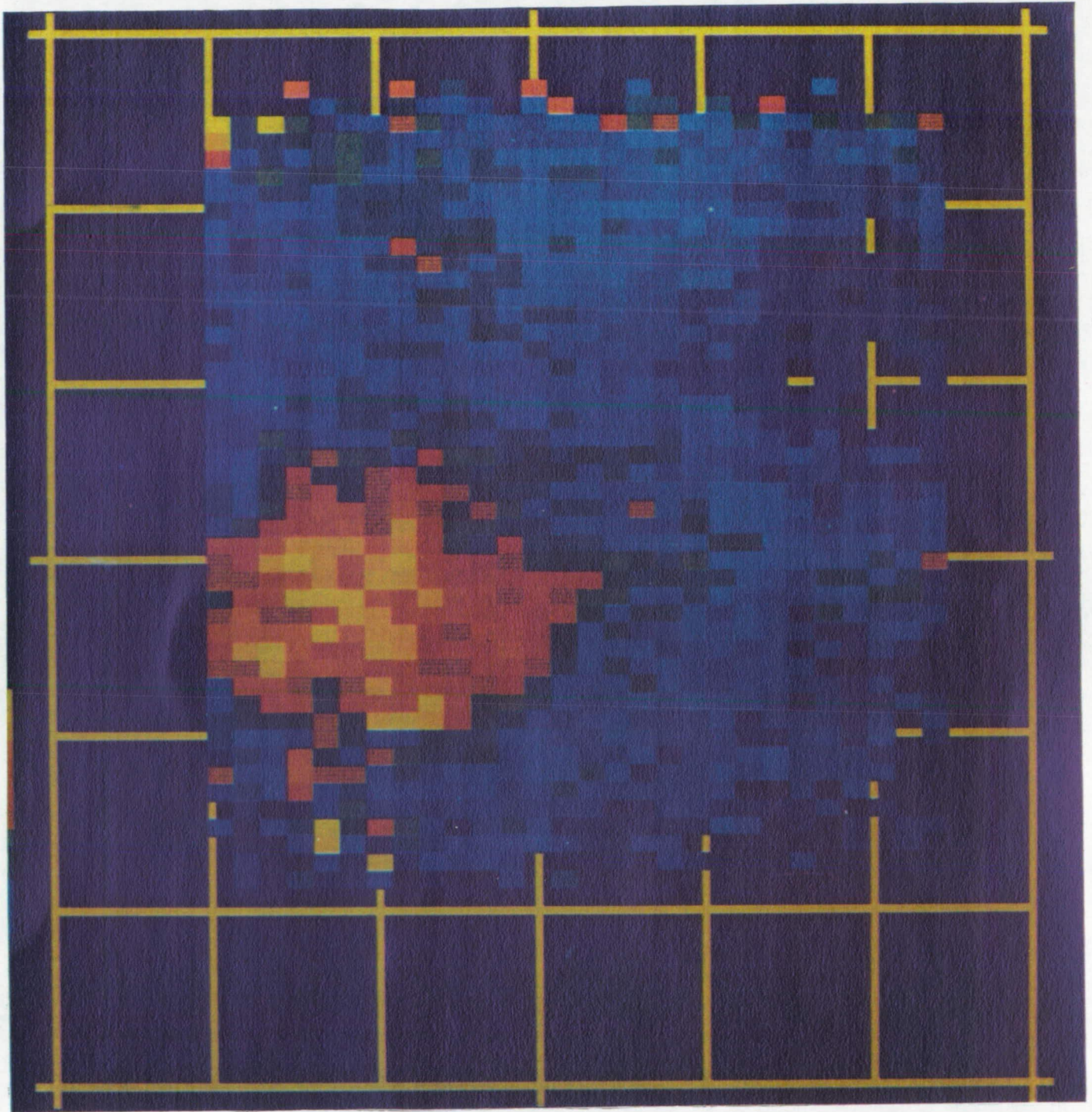


Figure 3.12. Nitric oxide airglow on the nightside (ref. 52).

ORIGINAL PAGE IS
OF POOR QUALITY

PAGE 50 INTENTIONAL BLANK

51

ORIGINAL PAGE
COLOR PHOTOGRAPH

PRECEDING PAGE BLANK NOT FILMED

HORIZONTAL WIND VELOCITY VECTOR MAP

SPECIES OXYGEN

ALTITUDE = 170 KM.

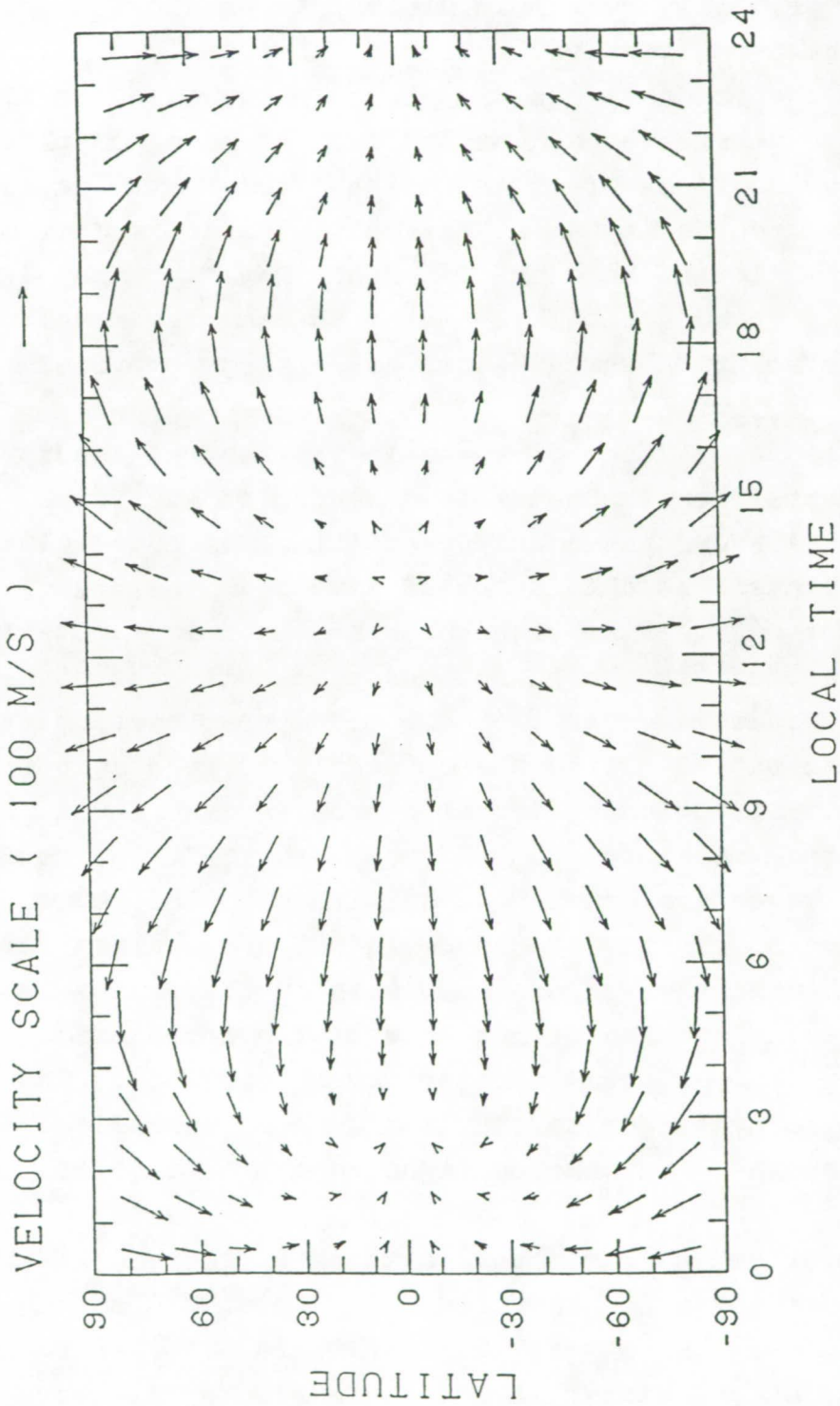


Figure 3.13. Horizontal wind flow from a spectral model of the thermosphere (ref. 47).

the flow across terminator. This lowers the nightside energy input due to adiabatic compressional heating which is balanced primarily by the 15 micron carbon dioxide cooling and, at higher altitudes, by conduction. Rayleigh friction is added to the momentum equation which slows down the flow across the terminator and amount of heat being supplied to the nightside. The effect is assigned to gravity waves which propagate upwards, break at high altitude and modify the horizontal flow. Like eddy diffusion, Rayleigh drag is treated as an adjustable parameter to make the model results match the solution which nature has already provided.

There is evidence of waves in the neutral density measurements from the neutral mass spectrometer (ref. 54). Figure 3.14 shows the density variation, with the altitude effect removed, as a function of time near the dusk terminator. Wave-like structures are seen in the various gases measured with helium out of phase with the other species. The waves travel slowly and appear stationary with respect to the satellite speed (nearly 10 km/s at periapsis). The actual direction of travel cannot be determined. A gravity wave model for the thermosphere (ref. 55) confirms that the waves are gravity waves with a period between 1/2 to 1 hour and an excitation source in the lower atmosphere. Higher frequency waves are also seen in the plasma near the region of the terminator but show little correlation with the lower frequency neutral density waves (ref. 56). The peak in the wave activity for carbon dioxide occurs near the terminator where turbulence might be expected (refs. 54,46).

Longer period waves have also been observed in the temperature deviations deduced from infrared observations at 90 km and drag density at 115 km (Figure 3.15) (ref. 57). The measurements differ in longitude by a little more than 180 degrees and are apparently in phase with each other. The

PV ONMS

NEUTRAL DENSITY GRAVITY WAVES

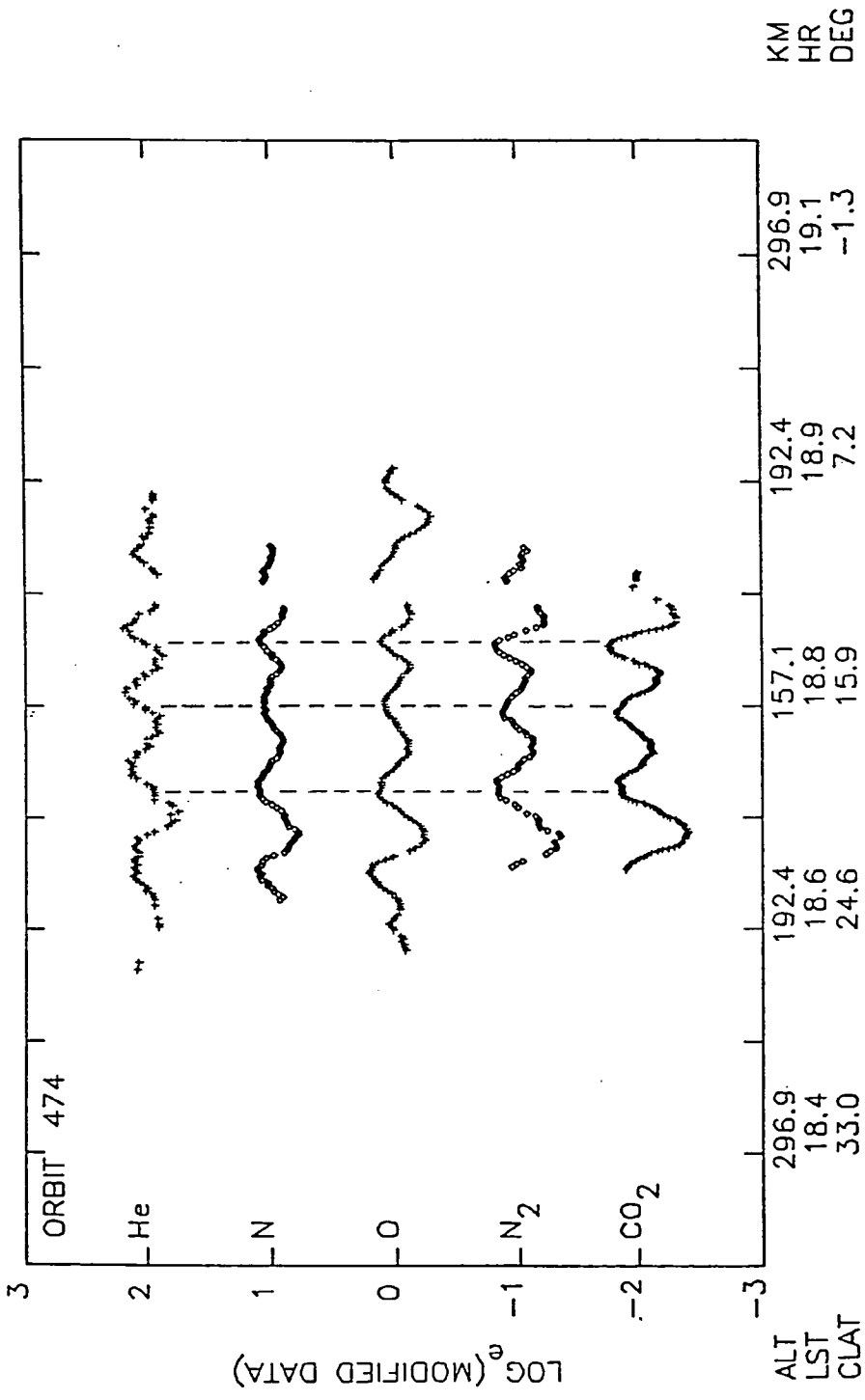


Figure 3.14. Wave-like perturbations in the neutral density (ref. 54).

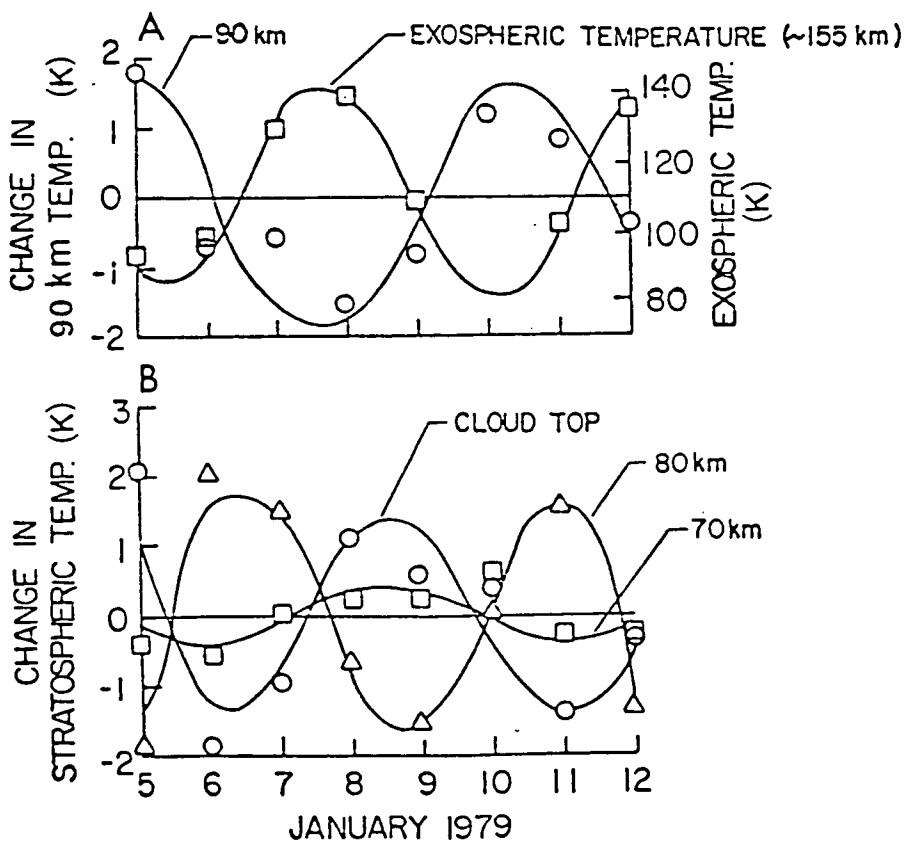
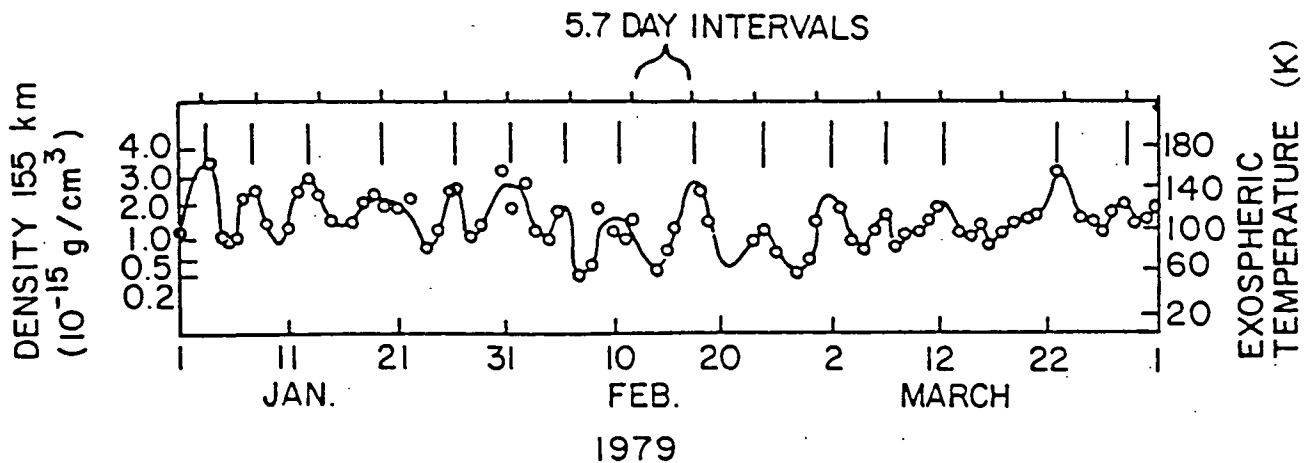


Figure 3.15. Inferred temperature variations at 90 km and 155 km (ref. 57).

period is about 5.6 days. It is thought that the perturbations are caused by planetary scale waves propagating upward from the lower atmosphere (ref. 28c).

4. IONOSPHERE/SOLAR WIND INTERACTION

Figure 4.1 (ref. 36c) shows the relative ion composition during daytime measured by the ion mass spectrometer. Note that the major ions are atomic oxygen and molecular oxygen not carbon dioxide. This is due to ion chemistry as is shown in Figure 4.2 (ref. 27f,71). Carbon dioxide ions are rapidly converted to atomic oxygen and molecular oxygen ions through atom-ion interchange or charge transfer. Dissociative recombination restores the neutral species. Ions can also participate in other neutral reactions (ref. 27e,71). For example, the charge exchange of hot protons with neutral H in the hydrogen bulge can lead to thermally excited neutral hydrogen atoms forming a hydrogen corona with some atoms having enough energy to escape. Other neutral reactions can also contribute the hydrogen corona. An oxygen corona is formed from the dissociative recombination of O_2^+ . Atomic oxygen atoms can also be ionized or photoionized, picked up by the local magnetic field, and transported elsewhere on the planet or in some cases even escape.

Coronas are observed (ref. 36b) in H, C, N and O (Figure 4.3). As can be seen for O the non-thermal or "hot" oxygen corona forms an extended atmosphere at high altitudes which is important for mass loading of the solar wind (refs. 7,58). In mass loading, "hot" oxygen is photoionized and gets attached to the solar wind magnetic field, slowing it down. Although "hot" hydrogen is also present in large concentrations, it is the more massive oxygen atom that is important for the process of mass loading. The data in the figure reflects solar maximum conditions.

Figure 4.4 (refs. 59,65) shows the solar wind interaction with the ionosphere of Venus. The solar wind is a low density plasma, 10 to 15 particles/cc, primarily

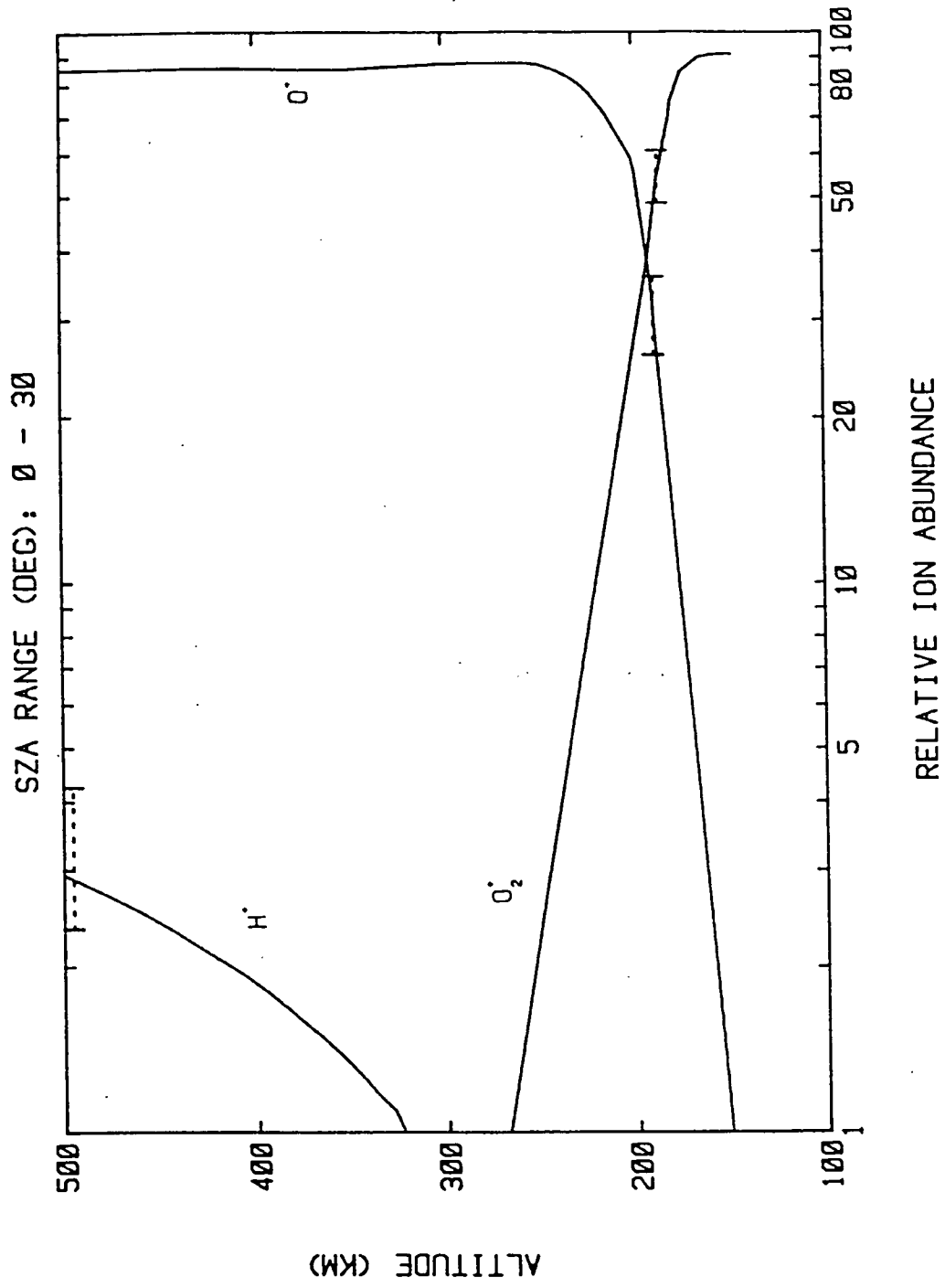
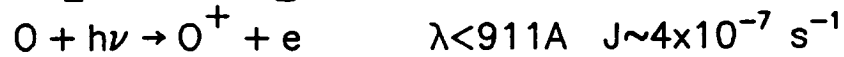
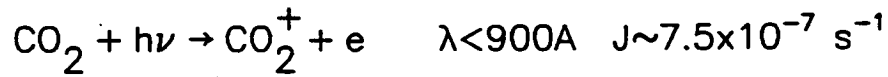


Figure 4.1. Relative ion composition during daytime (ref. 36c).

ION COMPOSITION (O_2^+ , O^+ MAJOR IONS)

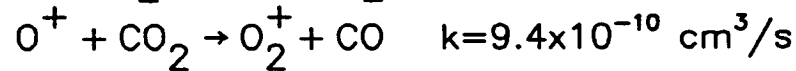
PRODUCTION



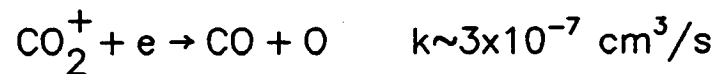
ATOM-ION INTERCHANGE



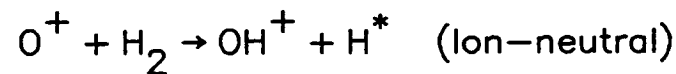
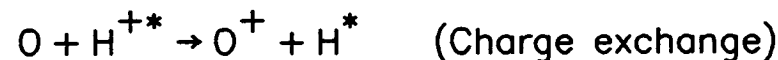
or CHARGE TRANSFER



DISSOCIATIVE RECOMBINATION



H: CORONA/ESCAPE



O: CORONA



SOLAR WIND PICKUP

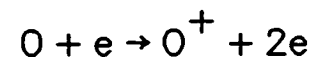


Figure 4.2. Various ion processes (refs. 27f, 71).

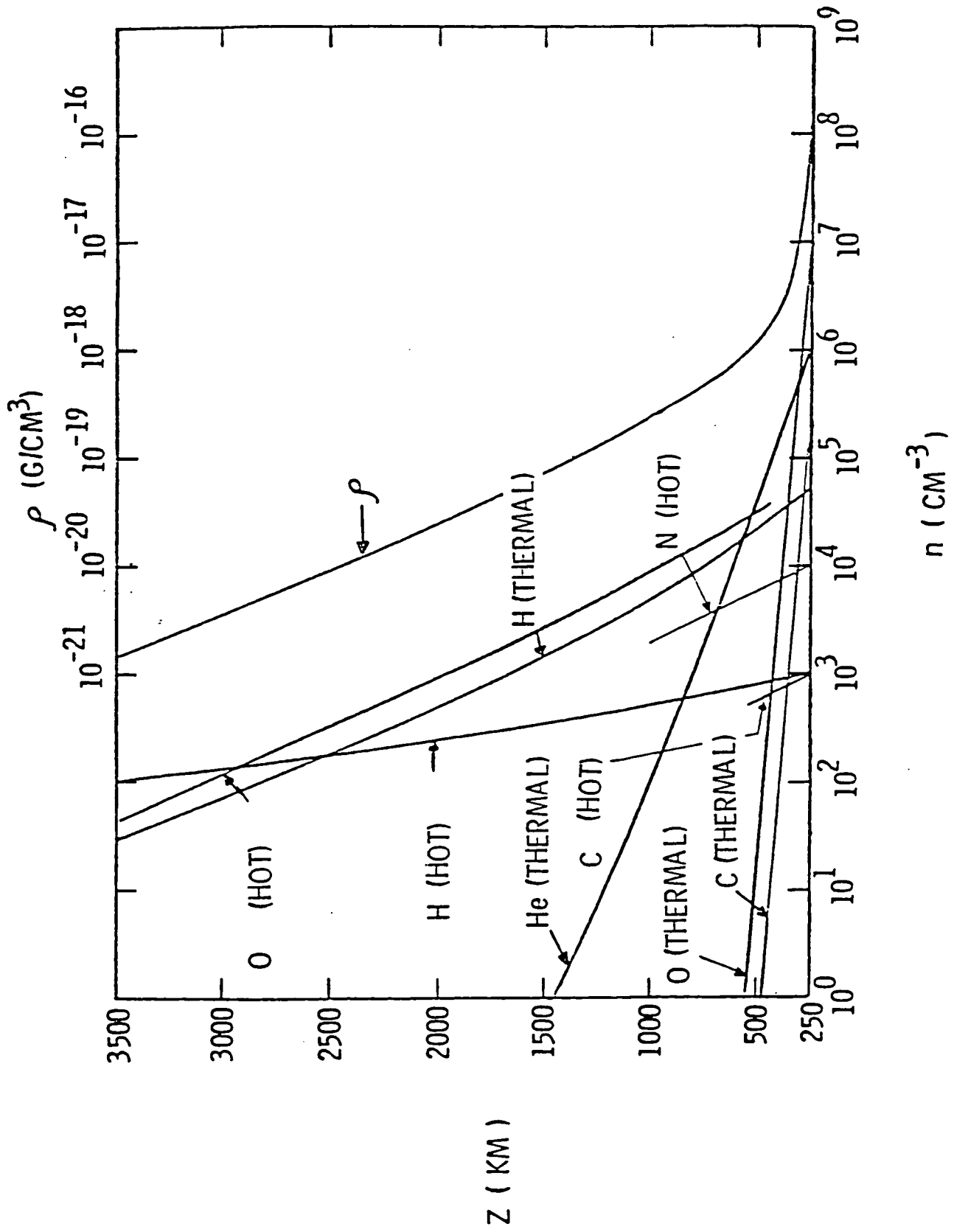


Figure 4.3. The coronas of H, C, N and O as a function of altitude (ref. 36b).

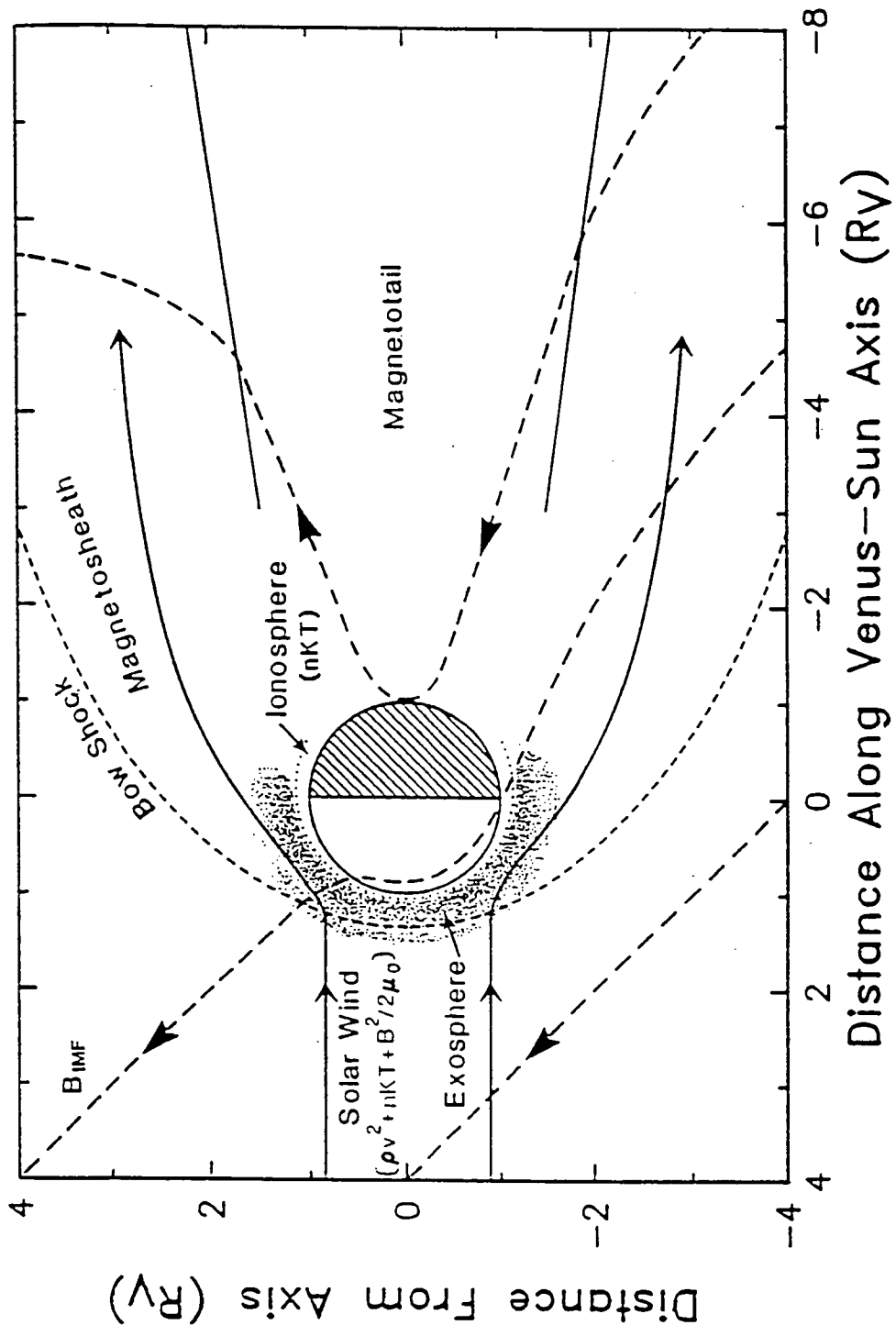


Figure 4.4. The solar wind interaction with Venus (ref. 59).

hydrogen, with a speed of about 400 km/s. The interplanetary magnetic field makes an angle of about 40 degrees with respect to a line connecting Venus and the Sun. The flow is supersonic, forming a bow shock about 1.3 radii of Venus at the sub-solar point. On earth the equivalent position is about 14-16 radii of Earth due to the presence of the Earth's magnetic field. The flow is turbulent across the the shock. The ionopause (ref. 69) is the boundary between the shocked solar wind and the ionosphere. It is approximately the balance point between the dynamic pressure of the solar wind and the ionospheric pressure. At the sub-solar point the ionopause is around 300 km. The mass loading is a maximum around 400 km (ref. 58) and the effect is to make the bow shock move outward (ref. 60,72).

5. SOLAR ACTIVITY EFFECTS

The effect of periapsis moving upward is shown in Figure 5.1 (ref. 61). There are several consequences of this fact: a) it is no longer possible to measure the neutral atmosphere and main ionosphere at low altitude; b) the nightside ionosphere is sampled at higher altitudes in a region termed the iontail; and c) the solar activity changes from solar maximum to solar minimum conditions as indicated by an EUV index derived from the electron temperature probe (refs. 60,69). The EUV index is a photo emission measurement (ref. 70) for wavelengths less than about 1300 Angstroms. A little more than one-half of the contribution comes from the Lyman-alpha line. Wavelengths in this range are responsible for heating and ionization of the atmosphere. The corresponding 10.7 cm radio flux index is about 200 at solar maximum and 70 at solar minimum (ref. 69).

The bowshock position as a function of solar activity is illustrated in Figure 5.2 (ref. 60). The position is measured at the terminator since the sub-solar point is not accessible at solar minimum due to the high altitude of periapsis. As solar activity decreases the terminator altitude moves inward (top). The actual distance is plotted in the bottom of the figure. The cause of this decrease is the decrease in the mass loading. At lower solar activity, the dissociative recombination of O_2^+ decreases due to the lower EUV input, resulting in a decrease in the "hot" oxygen corona and in the mass loading. There is also a decrease in the ionosheath or magnetosheath pressure near the terminator allowing the solar wind magnetic field to move closer to the planet. There is evidence that the atomic oxygen emission deduced from the 130.4 nanometer line has decreased from solar maximum to solar minimum as observed by the ultraviolet spectrometer (Figure 5.3) (ref. 1d). The emission, including both cold

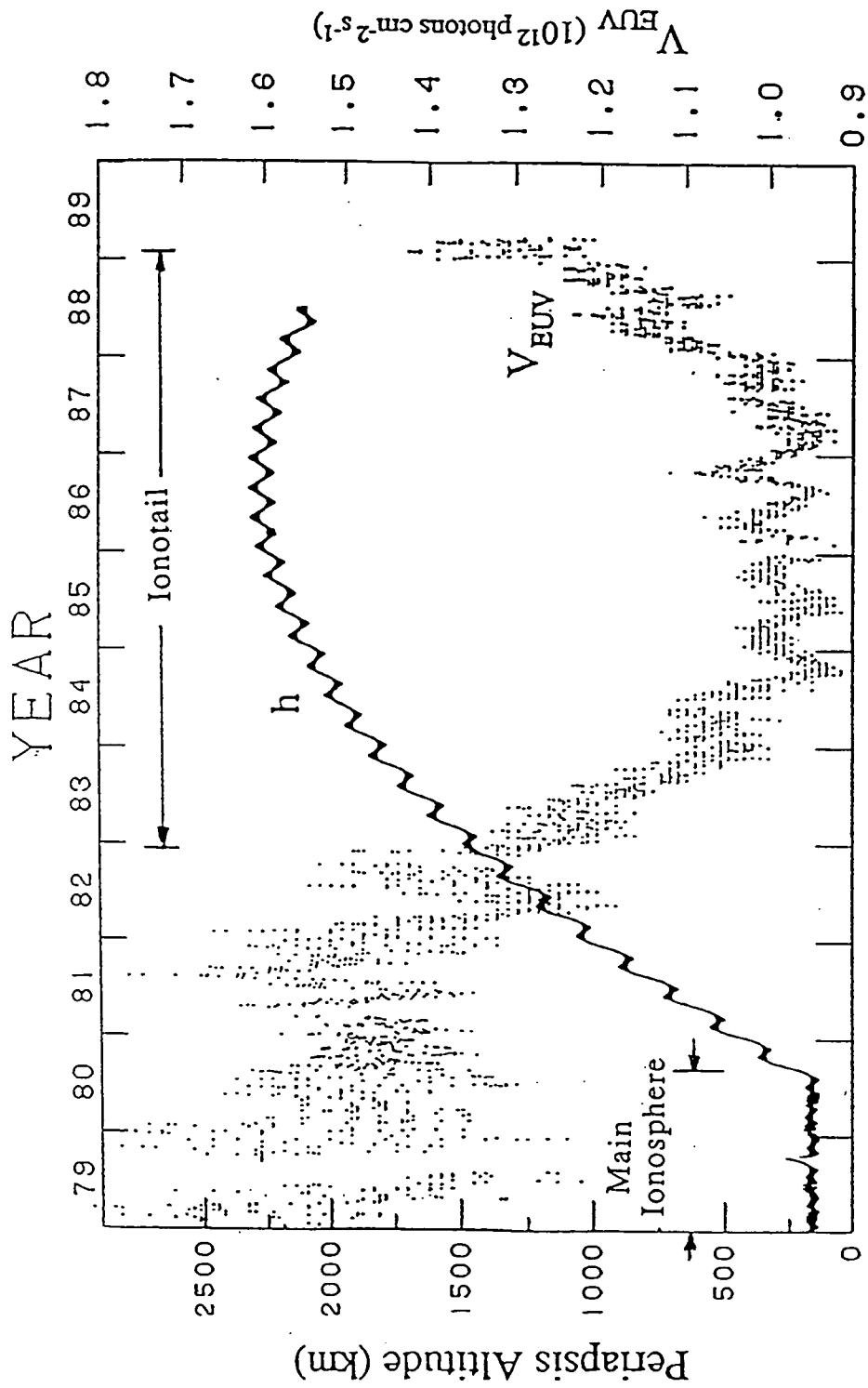


Figure 5.1. The periapisis altitude and solar activity EUV index as a function of year (ref. 61).

Solar Cycle Effects on Venus' Bow Shock

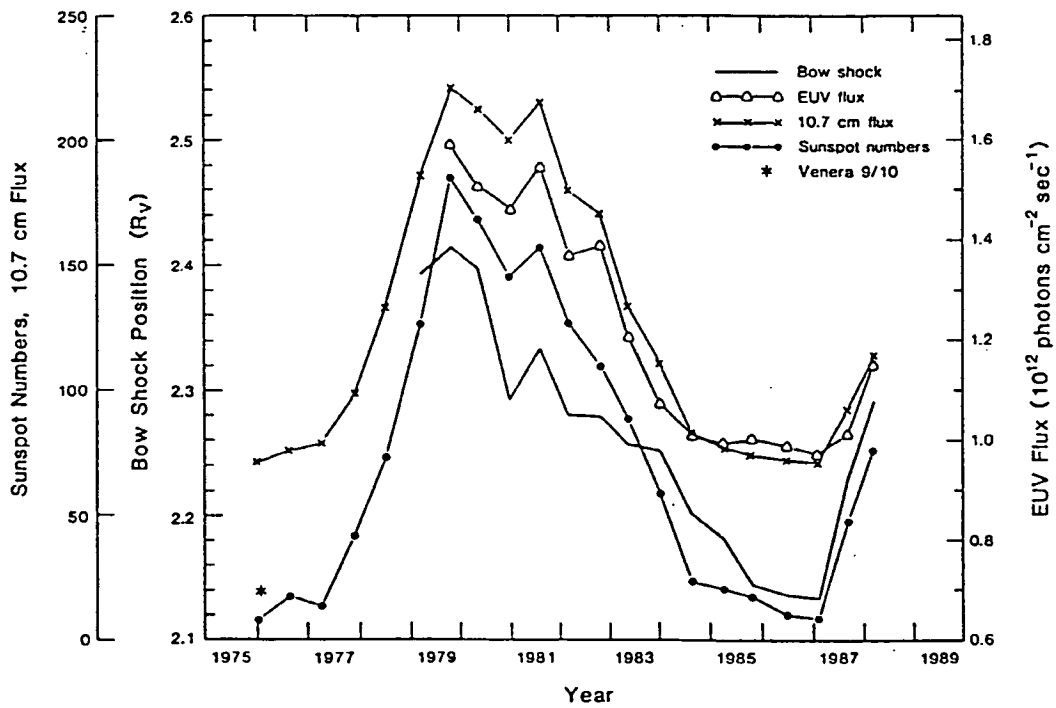
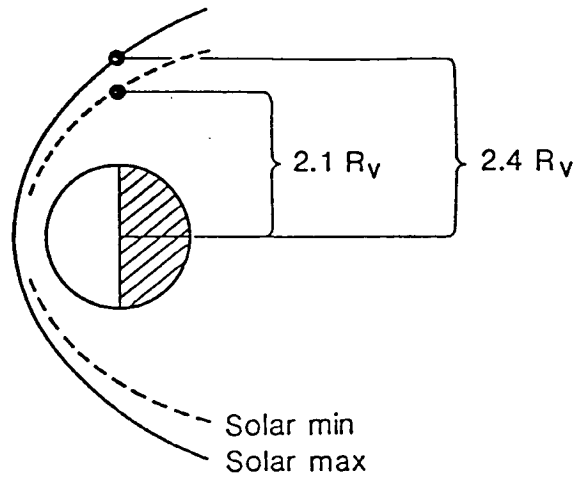


Figure 5.2. The bow shock position as a function of solar activity (ref. 60).

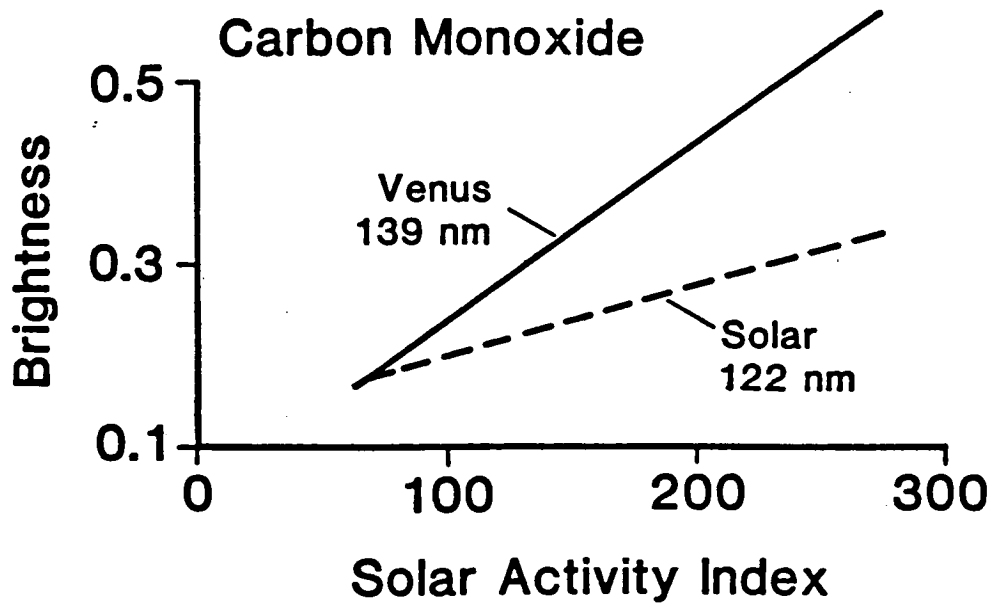
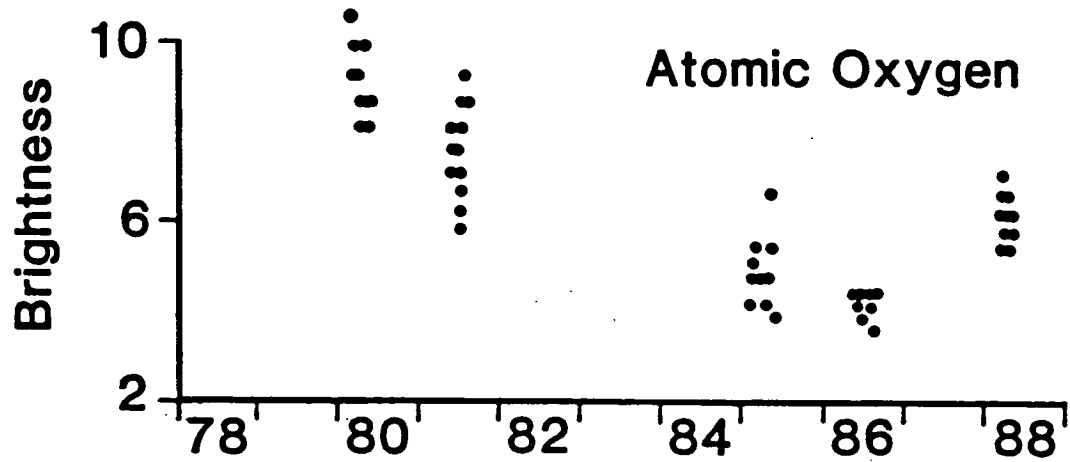


Figure 5.3. Atomic oxygen and carbon monoxide emission as a function of year and solar activity (ref. 1d).

and "hot" oxygen contributions, implies a decrease in the oxygen corona and in the mass loading.

Figure 5.4 shows the various processes occurring in the ionosphere of Venus (ref. 69): the bow shock and its interaction with the ionosphere; the formation of ions on the dayside, transport across the terminator; and subsistence or escape (ref. 62) on the nightside. The nightside is very erratic with two more or less permanent features called ionospheric holes or troughs. Two example orbits are shown in 1980 (solar maximum) and in 1986 (solar minimum). At solar minimum the nightside ionosphere at high altitude ("iontail") is sampled. In this region atomic oxygen ions of suprathermal energy (9-16 eV) and higher energies (greater than 40 eV) have been observed with enough energy to escape Venus (ref. 62).

The average electron density in the nightside iontail region (1400 to 2500 km) is shown in Figure 5.5. The average for each nightside tail pass is plotted along with the average EUV index (ref. 61). As solar activity decreases, the average electron density decreases. The relative roles of the variation with solar EUV, solar wind pressure change, transport across the terminator and the nightside ionization source is not clearly understood. At solar maximum transport across the terminator from the dayside to nightside is sufficient to maintain the nightside against loss due to recombination (ref. 28j). At solar minimum the situation is less clear and it may be that nightside ionization sources are relatively more important. Two possible sources have been identified: a) a 10-50 eV electron flux whose source is most likely the solar wind; and b) a downward flux of O⁺.

The electron flux is most likely responsible for the nightside aurora seen in atomic oxygen at 130.4 nm (ref. 6).

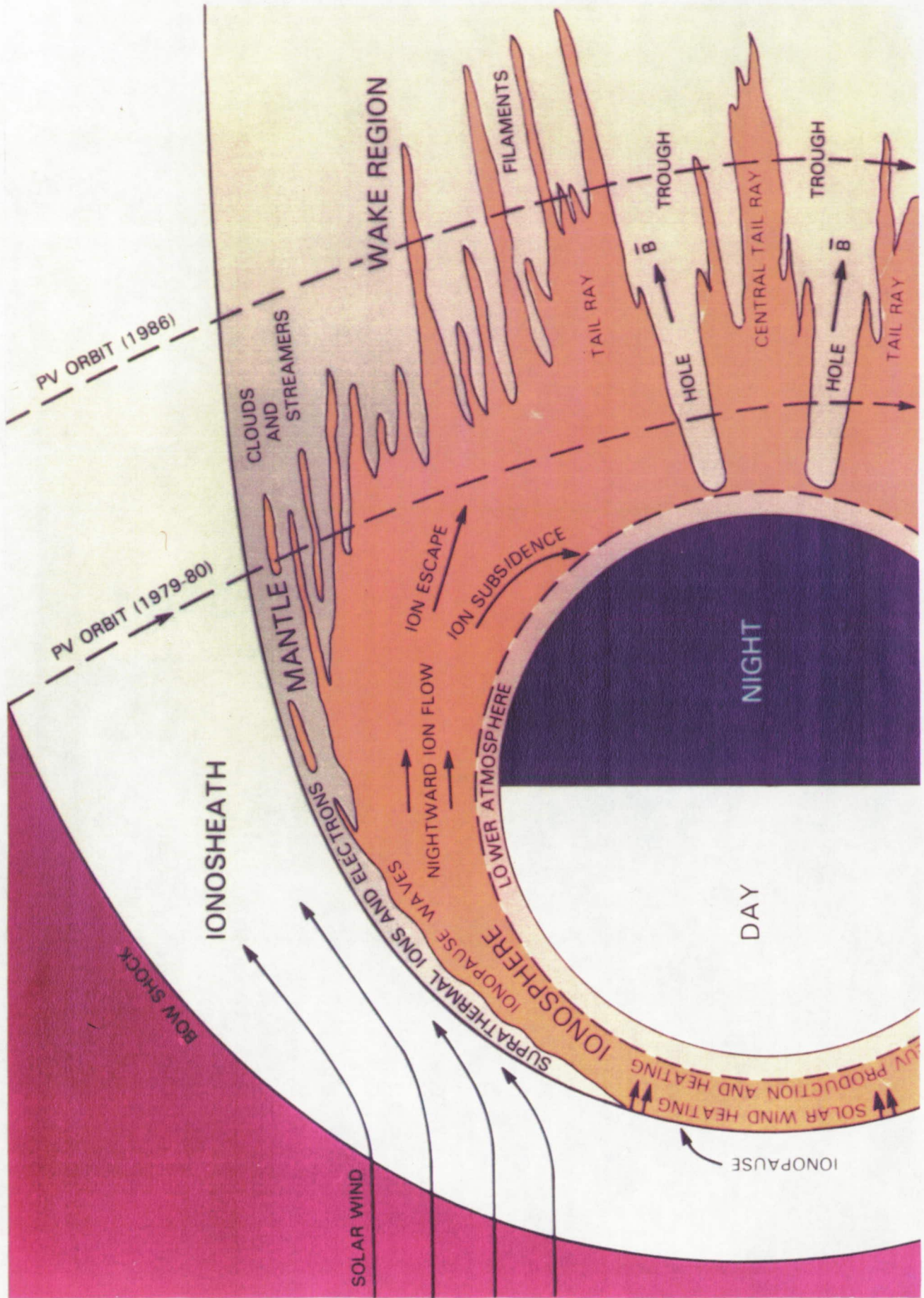


Figure 5.4. The various processes occurring in the ionosphere of Venus (ref. 69).

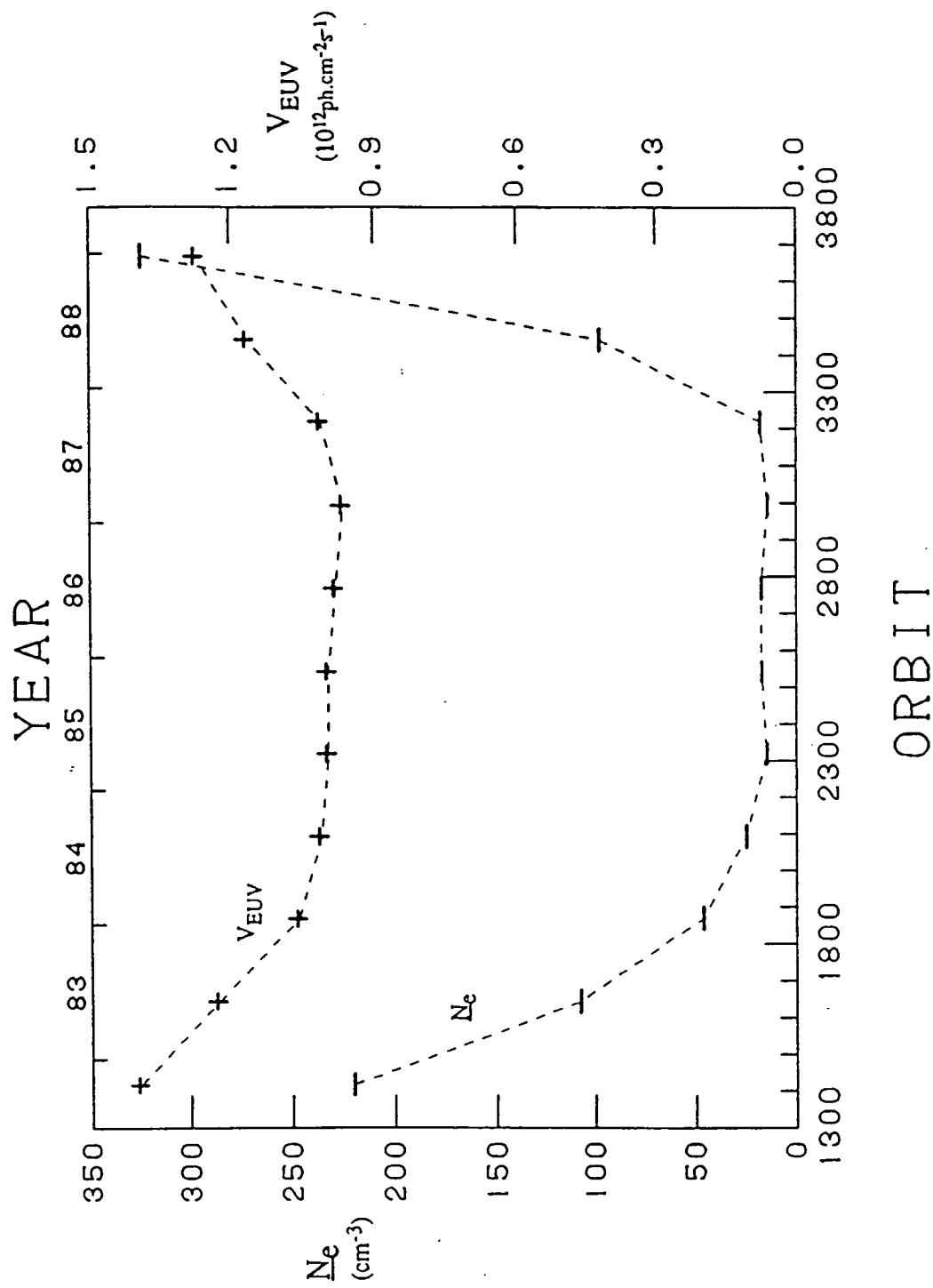


Figure 5.5. The average electron density as a function of solar activity (ref. 61).

The auroras are shown in Figure 5.6 for 3 different days. The crescent at the top of each image is due to the dayside resonant scattering of sunlight and photoelectron emission. The aurora on the nightside is highly variable as can be seen from the variation in emission intensity.

Although in situ measurements of the low altitude ionosphere are not possible at solar minimum, due to the high periapsis altitude, radio occultation measurements can be used to probe this region. Electron density profiles for 1980, at solar maximum, and in 1986, at solar minimum, are shown in Figure 5.7 (ref. 63). The peak density dropped by about a factor of 1.5 from solar maximum to solar minimum implying that the solar euv ionization source was reduced by about a factor of two. Photochemical equilibrium holds below about 180 km and in this case radio occultation measurements can be used to infer the neutral temperature above the ion peak near 140 km (ref. 64). The solar maximum minus minimum exospheric temperature change is about 60 K (ref. 64), that from empirical models (refs. 45,36b) about 55 to 70 K and that from theoretical models (refs. 66,67) about 65 to 70 K. However, all of these changes are smaller than that observed for the Earth's thermosphere (ref. 68) of about 420 K. Clearly the Venus exospheric temperature is less sensitive to solar cycle change than the Earth. The strong 15 micron cooling due carbon dioxide buffers the response of the exosphere to changes in the solar euv activity (ref. 67).

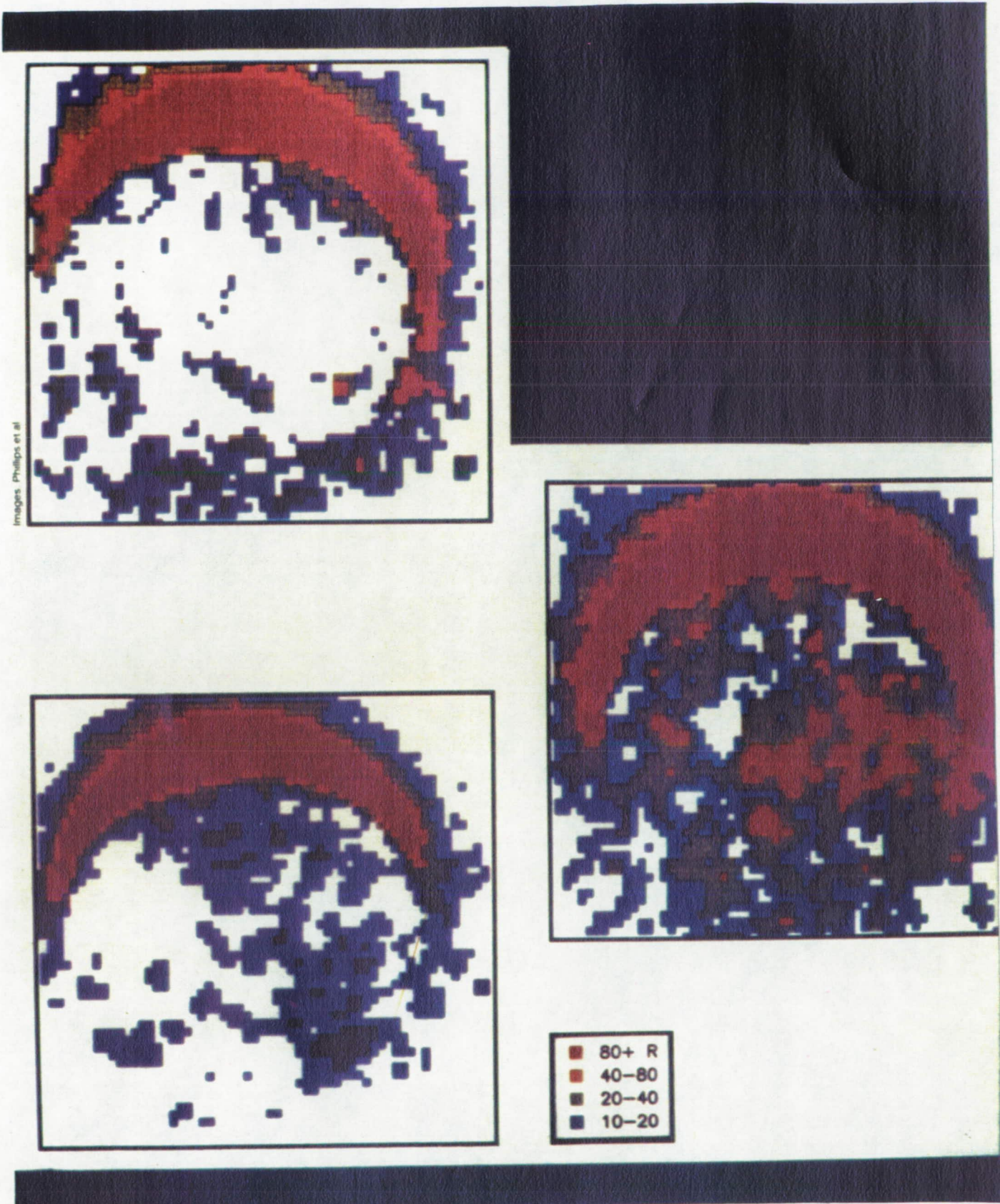


Figure 5.6. Nightside atomic oxygen aurora (ref. 6).

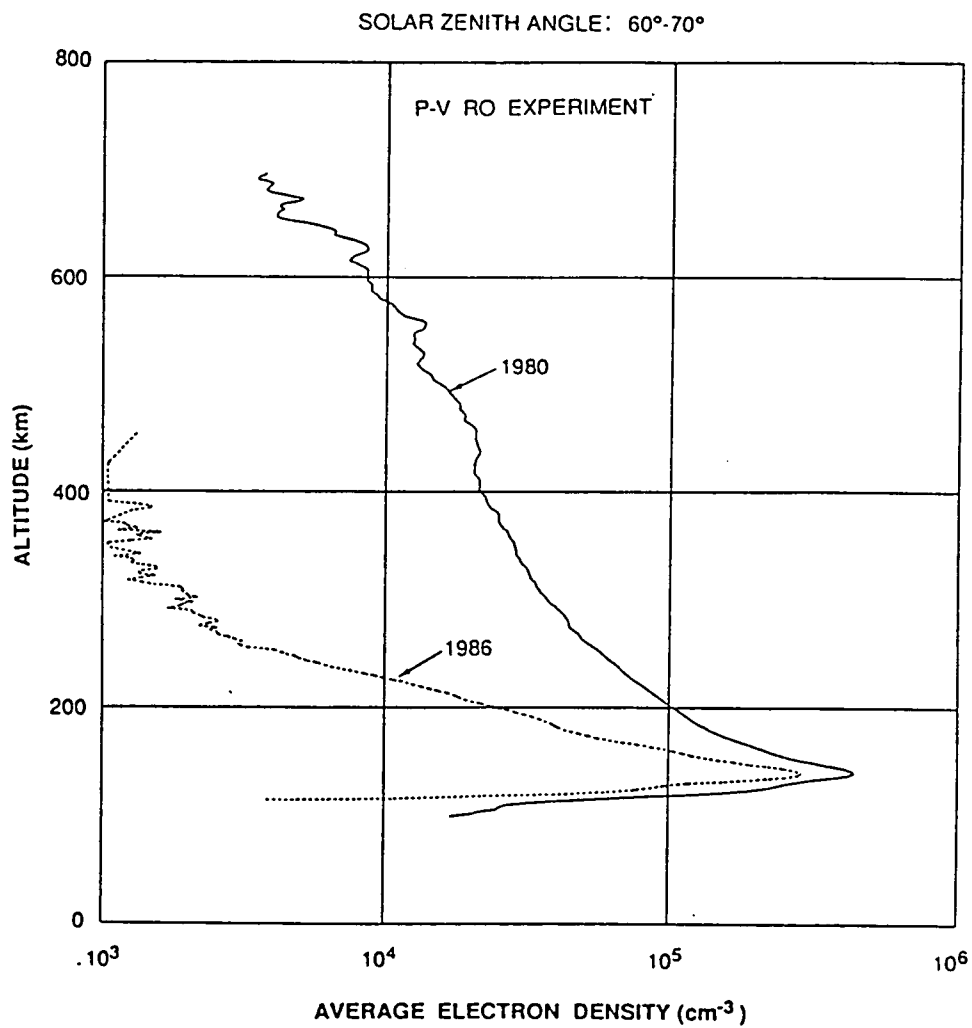


Figure 5.7. Electron density profiles from radio occultation (ref. 63).

Table 5.1. Neutral Exospheric Temperature Change at Solar Maximum and Solar Minimum Conditions

NEUTRAL EXOSPHERE TEMPERATURE

- $\Delta T = T(\text{Solar maximum}) - T(\text{Solar minimum})$

Radio Occultation	$\Delta T = 60\text{K}$	(150 km, SZA=55°–75°)
Hedin et al. empirical model	$\Delta T_{\infty} = 55\text{K}$	($F_{10.7} = 200$ to 70)
VIRA empirical model	$\Delta T_{\infty} = 75\text{K}$	($F_{10.7} = 200$ to 70)
Dickenson & Bougher 1-D	$\Delta T_{\infty} = 65\text{K}$	($F_{10.7} = 200$ to 74)
NCAR-2D	$\Delta T_{\infty} = 70\text{K}$	($F_{10.7} = 200$ to 74)
EARTH (MSIS)	$\Delta T_{\infty} = 420\text{K}$	($F_{10.7} = 200$ to 70)

- Venus temperature less sensitive to solar cycle change than Earth
- NCAR model results at solar minimum compared to maximum:
 - Reduced EUV ($\lambda < 105$ nm) inputs by factor of 3
 - Reduced 15- μm cooling; reduced wind speed (20–30 m/s)
 - Reduced NO (δ band) night airglow by factor of 3
 - Night side temperature about same; minimum at 0200 hours LST

6. SUMMARY

A large body of data has been accumulated on Venus, its atmosphere and ionosphere by the Pioneer Venus Orbiter. The data base now covers almost an entire solar cycle. The reentry period 1992 will allow further measurements of the neutral atmosphere and low altitude ionosphere. At the end of this time the Orbiter will fade away to a well deserved rest after having performed its tasks as a good and faithful servant.

REFERENCES

- 1a. Colin, L., 1989, Pioneer Venus Orbiter - Ten Years of Discovery, ed. L. Colin, NASA/Ames Research Center, Table 2.
- 1b. Sjogren, J., 1989, Pioneer Venus Orbiter -Ten Years of Discovery, ed. L. Colin, NASA/Ames Research Center, Chapter 4.6.2 (The Surface and the Interior: Gravity Field).
- 1c. Hunten, D.M., 1989, Pioneer Venus Orbiter -Ten Years of Discovery, ed. L. Colin, NASA/Ames Research Center Chapter, 4.7 (Venus: Lessons for Earth).
- 1d. Stewart, A.I.F., 1989, Pioneer Venus Orbiter - Ten Years of Discovery, ed. L. Colin, NASA/Ames Research Center, Chapter 4.5 (The Atmosphere Seen from Orbit).
- 1e. Brace, L.H., 1989, Pioneer Venus Orbiter -Ten Years of Discovery, ed. L. Colin, NASA/Ames Research Center, Chapter 4.3 (The Dynamics of the Ionosphere).
- 1f. Colin, L., 1989, Pioneer Venus Orbiter - Ten Years of Discovery, ed. L. Colin, NASA/Ames Research Center, Tables 7.0.1,8.0.1.
- 2a. Fimmel, R.O., L. Colin and E. Burgess, 1983, Pioneer Venus, NASA SP-461, NASA Scientific and Technical Information Branch, Chapter 2.
- 2b. Fimmel, R.O., L. Colin and E. Burgess, 1983, Pioneer Venus, NASA SP-461, NASA Scientific and Technical Information Branch, Chapter 8.
- 2c. Fimmel, R.O., L. Colin and E. Burgess, 1983, Pioneer Venus, NASA SP-461, NASA Scientific and Technical Information Branch, Chapter 6.
3. Colin, L., 1989, Pioneer Venus Bibliography, Pioneer Missions Office, Ames Research Center, Moffett Field Calif.
4. Beatty, J.K., 1978 "Encounters with Venus," Sky and Telescope, 56(6), pp. 484-486.
5. Eberhart, J., 1986, "The Night Skies of Venus: Another Kind of Aurora," Eberhart, Science News, 130(25), pp. 364-365.

6. Phillips, J.L., A.I.F. Stewart and J.G. Luhman, 1986, "The Venus Ultraviolet Aurora: Observations at 130.4 NM," Geophysical Research Letters, 13(10), pp. 1047-1050.
7. Luhmann, J.G., 1986, "The Solar Wind Interaction with Venus," Space Science Reviews, 44, pp. 241-306.
- 8a. Meszaros, S.P., 1983, Planetary Size Comparisons: A Photographic Study, NASA TM-85017, NASA photo number 83H228, p. 2-30.
- 8b. Meszaros, S.P., 1983, Planetary Size Comparisons: A Photographic Study, NASA TM-85017, NASA photo number 83HC206, p. 2-31.
9. Phillips, J.L. and C.T. Russell, 1987, "Upper Limit on the Intrinsic Magnetic Field of Venus," Journal of Geophysical Research, 92(A3), pp. 2253-2263.
10. Parker, E.N., 1983, "Magnetic Fields in the Cosmos," Scientific American, 249(2), pp. 44-54.
11. Stevenson, D.L., T. Spohn, and G. Schubert, 1983, "Magnetism and Thermal Evolution of the Terrestrial Planets," Icarus, 54, pp. 466-489.
12. Pettengill, G.H., D.B. Campbell and H. Masursky, 1980, "The Surface of Venus," Scientific American, 243(2), pp. 54-65.
13. Masursky, H., E. Eliason, P.G. Ford, G.E. McGill, G.H. Pettengill, G.G. Schaber and G. Schubert, 1980, "Pioneer Venus Radar Results: Geology from Images and Altimetry," Journal of Geophysical Research, 85(A13), pp. 8232-8260.
14. "Fractured Aphrodite," 1987, Scientific American, 257(1), p. 19.
15. Saunders, R.S. and M.H. Carr, 1984, "VENUS," in Geology of the Terrestrial Planets, NASA SP-469, pp. 57-77.
16. Briggs, G. and F. Taylor, 1986, "VENUS," in Cambridge Photographic Atlas of the Planets, Cambridge University Press, pp. 44-71.

17. Greely, R., 1985, "VENUS," in Planetary Landscapes, Allen and Unwin, pp. 132-260.
18. Burgess, E., 1985, VENUS, Columbia University Press, N.Y., Chapter 6.
19. Beatty, J.K., 1982, "VENUS: The Mystery Continues," Sky and Telescope, 63(2), pp. 134-138.
20. Meszaros, S.P., 1982, Planets and Moons of the Solar System as Viewed by NASA Spacecraft, Goddard Space Flight Center Library, NASA photo number 79HC46.
21. Bazilevskiy, A.T., 1989, "The Planet Next Door," Sky and Telescope, 77(4), pp. 360-368.
22. "The Stuff of Venus: Taste-tests and Turmoil", 1982, Science News, 121(13), pp. 214-215.
23. "The Basalts of Venus", 1983, Scientific American, 249(2), pp. 58-59.
24. "The Other Side of Venera 14: Capturing Venusian Evolution?," 1982, Science News, 121(15), p. 245.
25. J. Eberhart, 1982, "Eyes on Venus: A New Dimension", Science News, 121(15), pp. 248-249.
26. Pieters, C.M., J.W. Head, W. Patterson, S. Pratt, J. Garvin, V.L. Barsukov, A.T. Basilevsky, I.L. Khodakovsky, A.S. Selivanov, A.S. Panfilov, Y.M. Gektin and Y.M. Narayeva, 1986, "The Color of the Surface of Venus," Science, 234, pp. 1379-1383.
- 27a. Chamberlain, J.W. and D.M. Hunten, 1987, Theory of Planetary Atmospheres, Academic Press Inc., San Diego Ca., Chapter 1 (Vertical Structure of the Atmosphere).
- 27b. Chamberlain, J.W. and D.M. Hunten, 1987, Theory of Planetary Atmospheres, Academic Press Inc., San Diego Ca., Chapter 4 (Planetary Astronomy).
- 27c. Chamberlain, J.W. and D.M. Hunten, 1987, Theory of Planetary Atmospheres, Academic Press Inc., San Diego Ca., Chapter 6 (Airglow, Auroras, Aeronomy).

- 27d. Chamberlain, J.W. and D.M. Hunten, 1987, Theory of Planetary Atmospheres, Academic Press Inc., San Diego Ca., Chapter 2 (Hydromatics of Atmospheres).
- 27e. Chamberlain, J.W. and D.M. Hunten, 1987, Theory of Planetary Atmospheres, Academic Press Inc., San Diego Ca., Chapter 7 (Stability of Planetary Atmospheres).
- 27f. Chamberlain, J.W. and D.M. Hunten, 1987, Theory of Planetary Atmospheres, Academic Press Inc., San Diego Ca., Chapter 5 (Ionosphere).
- 28a. Hunten, D.M., 1983, in Venus, ed. D.M. Hunten, L. Colin, T.M. Donahue and V.I. Moroz, University of Arizona Press, Tucson Az., pp. vii-viii.
- 28b. von Zahn, U., S. Kumar, H. Niemann, R. Prinn, "13. The Composition of the Venus Atmosphere," 1983, in Venus, ed. D.M. Hunten, L. Colin, T.M. Donahue and V.I. Moroz, University of Arizona Press, Tucson Az., pp. 299-430.
- 28c. Schubert, G., "21. The General Circulation and the Dynamical State of the Venus Atmosphere," 1983, in Venus, ed. D.M. Hunten, L. Colin, T.M. Donahue and V.I. Moroz, University of Arizona Press, Tucson Az., pp. 681-765.
- 28d. Taylor, F.W., D.M. Hunten, and L.V. Ksanfomaliti, "20. The Thermal Balance of the Middle and Upper Atmosphere," 1983, in Venus, ed. D.M. Hunten, L. Colin, T.M. Donahue and V.I. Moroz, University of Arizona Press, Tucson Az., pp. 650-680.
- 28e. Tomasko, M.G. "18. The Thermal balance of the Lower Atmosphere of Venus," 1983, in Venus, ed. D.M. Hunten, L. Colin, T.M. Donahue and V.I. Moroz, University of Arizona Press, Tucson Az., pp. 604-631.
- 28f. Phillips, R.J. and M.C. Malin, 1983, "10. The Interior of Venus and Tectonic Implications," in Venus, ed. D.M. Hunten, L. Colin, T.M. Donahue and V.I. Moroz, University of Arizona Press, Tucson Az., pp. 159-214.

- 28g. Moroz, V.I., 1983, "5. Summary of Preliminary Results of the Venera 13 and Venera 14 Missions," in Venus, ed. D.M. Hunten, L. Colin, T.M. Donahue and V.I. Moroz, University of Arizona Press, Tucson Az., pp. 45-68.
- 28h. Seiff, A., 1983, "11. Thermal Structure of the Atmosphere," in Venus, ed. D.M. Hunten, L. Colin, T.M. Donahue and V.I. Moroz, University of Arizona Press, Tucson Az., pp. 215-279.
- 28i. Colin, L., 1983, "2. Basic Facts," in Venus, ed. D.M. Hunten, L. Colin, T.M. Donahue and V.I. Moroz, University of Arizona Press, Tucson Az., pp. 10-26.
- 28j. Brace, L.H., H.A. Taylor, T.I. Gambosi, A.J. Kliore, W.C. Knudsen and A.F. Nagy, 1983, "23. The Ionosphere of Venus: Observations and their Interpretation," in Venus, ed. D.M. Hunten, L. Colin, T.M. Donahue and V.I. Moroz, University of Arizona Press, Tucson Az., pp. 779-840.
29. Kastings, J.F., O.B. Toon and J.B. Pollack, 1988, "How Climate Evolved on the Terrestrial Planets," Scientific American, 258(2), pp. 90-97.
30. Kastings, J.F., J.B. Pollack, and T.P. Ackerman, 1984, "Response of Earth's Atmosphere to Increases in Solar Flux and Implications for Loss of Water From Venus", Icarus, 57, pp. 335-355.
31. Kumar, S., D.M. Hunten, and J.B. Pollack, 1983, "Nonthermal Escape of Hydrogen and Deuterium from Venus and Implications for Loss of Water," Icarus, 55, pp. 369-389.
32. Donahue, T.M., J.H. Hoffman and R.R. Hodges, Jr., 1982, "Venus was Wet: A Measurement of the Ratio of D to H," Science, 216, pp. 630-633.
33. McElroy, M.B., M.J. Prather, and M.J. Rodriguez, 1982, "Escape of Hydrogen from Venus", Science, 215, pp. 1614-1615.
34. Hartle, R.E. and H.A. Taylor, 1983, "Identification of Deuterium Ions in the Ionosphere of Venus," Geophysical Research Letters, 10, pp. 965-968.

35. Pollack, J.B., O.B. Toon, and R. Boese, 1980, "Greenhouse Models of Venus' High Surface Temperature, as Constrained by Pioneer Venus Measurements," Journal of Geophysical Research, 85(A13), pp. 8223-8231.
- 36a. V.I. Moroz, A.P. Ekonomov, B.E. Moshkin, H.E. Revercomb, L.A. Sromovsky, J.T. Schofield, D. Spankuch, F.W. Taylor and M. Tomasko, 1985, "Solar and Thermal Radiation in the Venus Atmosphere," in Venus International Reference Atmosphere, ed. A.V. Kliore, V.I. Moroz and G.M. Keating, Advances in Space Research, 5(11), chapter 6.
- 36b. G.M. Keating, J.L. Bertaux, S.W. Bougher, T.E. Cravens, R.E. Dickenson, A.E. Hedin, V.A. Krasnopolsky, A.F. Nagy, J.Y. Nicholson, L.J. Paxton, and U. von Zahn, 1985, "Models of Venus Neutral Upper Atmosphere Structure and Composition," in Venus International Reference Atmosphere, ed. A.V. Kliore, V.I. Moroz and G.M. Keating, Advances in Space Research, 5(11), chapter 4.
- 36c. S.J. Bauer, L.M. Brace, H.A. Taylor, T.K. Breus, A.J. Kliore, W.C. Knudsen, A.F. Nagy, C.T. Russell and N.A. Savich, 1985, "The Venus Ionosphere," in Venus International Reference Atmosphere, ed. A.V. Kliore, V.I. Moroz and G.M. Keating, Advances in Space Research, 5(11), chapter 7.
37. Pollack, J.B., 1981, "Atmospheres of Terrestrial Planets," in The New Solar System, ed. J.K. Beatty, B. O'Leary, and A. Chaikin, Sky Publishing Corp., Cambridge Mass., pp. 57-70.
38. "Venus Atmospheric Circulation Described by Pioneer," 1981, NASA Activities, 12(9), p. 10.
39. "Balloons Over Venus", 1986, Scientific American, 254(5), p. 69.
40. "Venus Volcanism: Another Hint," 1989, Science News, 136(24), p. 383.
41. Schubert, G. and C. Covey, 1981, "The Atmosphere of Venus," Scientific American, 245(1), pp. 66-74.
42. Prinn, R.G., 1985, "The Volcanoes and Clouds of Venus", Scientific American, 252(3), pp. 46-53.

43. Knollenberg, R., L. Travis, M. Tomasko, P. Smith, B. Ragent, L. Esposito, D. McCleese, J. Martonchik, and R. Beer, 1980, "The Clouds of Venus: A Synthesis Report," Journal of Geophysical Research, 85(A13), pp. 8059-8081.
44. Woo, R., J.W. Armstrong and A. Ishimaru, 1980, "Radio Occultation Measurements of Turbulence in the Venus Atmosphere by Pioneer Venus," Journal of Geophysical Research, 85(A13), pp. 8031-8038.
45. Hedin, A.E., H.B. Niemann, W.T. Kasprzak and A. Seiff, 1983, "Global Empirical Model of the Venus Thermosphere," Journal of Geophysical Research, 88(A1), pp. 73-83. "Correction to 'Global Empirical Model of the Venus Thermosphere' by A.E. Hedin et al.," 1983, Journal of Geophysical Research, 88(A8), pp. 6352.
46. Niemann, H.B., W.T. Kasprzak, A.E. Hedin, D.M. Hunten, and N.W. Spencer, 1980, "Mass Spectrometric Measurements of the Neutral Gas Composition of the Thermosphere and Exosphere of Venus," Journal of Geophysical Research, 85(A13), pp. 7817-7827.
47. Mengel, J.G., D.R. Stevens-Rayburn, H.G. Mayr and I. Harris, 1989, "Non-Linear Three Dimensional Spectral Model of the Venusian Thermosphere with Super-Rotation--II. Temperature, Composition and Winds," Planetary Space Science, 37(6), pp. 707-722.
48. Mayr, H.G., I. Harris, R.E. Hartle, K.H. Schatten, H.A. Taylor, K.L. Chan and D.R. Stevens-Rayburn, 1985, "Conjecture on Superrotation in Planetary Atmospheres: A Diffusion Model with Mixing Length Theory," Advances in Space Research, 5(9), pp. 63-68.
49. Brinton, H.C., H.A. Taylor, H.B. Niemann, H.G. Mayr A.F. Nagy, T.E. Cravens and D.F. Strobel, 1980, "Venus Nighttime Hydrogen Bulge," Geophysical Research Letters, 7(11), pp. 865-868.
50. Paxton, L.J., D.E. Anderson, A.I.F. Stewart, 1985, "The Pioneer Venus Ultraviolet Spectrometer Experiment; Analysis of Hydrogen Lyman-Alpha Data," Advances in Space Research, 5(9), pp. 129-132.

51. Taylor, H.A., H.C. Brinton, S.J. Bauer, R.E. Hartle, P.A. Cloutier and R.E. Daniell, 1980, "Global Observations of the Composition and Dynamics of the Ionosphere of Venus: Implications for the Solar Wind Interaction," Journal of Geophysical Research, 85(A13), pp. 7765-7777.
52. Stewart, A.I.F., J.C. Gerard, D.W. Rusch and S.W. Bougher, 1980, "Morphology of the Venus Ultraviolet Night Airglow," Journal of Geophysical Research, 85(A13), pp. 7861-7870.
53. Bougher, S.W., R.E. Dickinson, E.C. Ridley, R.G. Roble, A.F. Nagy, and T.E. Cravens, 1986, "Venus Mesosphere and Thermosphere II. Global Circulation, Temperature, and Density Variations," Icarus, 68, pp. 284-312.
54. Kasprzak, W.T., A.E. Hedin, H.G. Mayr, and H.B. Niemann, 1988, "Wavelike Perturbations Observed in the Neutral Thermosphere of Venus," Journal of Geophysical Research, 93(A10), pp. 11237-11245.
55. Mayr, H.G., I. Harris, W.T. Kasprzak, M. Dube and F. Varosi, 1988, "Gravity waves in the Upper Atmosphere of Venus," Journal of Geophysical Research, 93(A10), pp. 11247-11262.
56. Hoegy, W.R., L.H. Brace, W.T. Kasprzak and C.T. Russell, 1990, "Small Scale Plasma, Magnetic and Neutral Density Fluctuations in the Nightside Venus Ionosphere," accepted for publication in Journal of Geophysical Research.
57. Keating, G.M., F.W. Taylor, J.Y. Nicholson and E.W. Hinson, 1979, "Short-Term Cyclic Variations and Diurnal Variations of the Venus Upper Atmosphere," Science, 205(4401), pp. 62-64.
58. "Magnetic fields in the Ionosphere of Venus", J.G. Luhman and T.E. Cravens, to be published in Space Science Reviews, 1990.
59. Phillips, J.L. and D.J. McComas, 1990, "The Magnetosheath and Magnetotail of Venus," to be published in Space Science Reviews.

60. Russell, C.T., E. Chiou, J.G. Luhmann and L.H. Brace, 1990, "Solar Cycle Variations in the Neutral Exosphere Inferred from the Location of the Venus Bow Shock," Advances in Space Research, 10(5), pp. (5)5-(5)9.
61. Brace, L.H., R.F. Theis and J.D. Mihalov, 1989, "Solar Wind and Solar Cycle Control of the Venus Nightside Upper Ionosphere," IAGA, Session 2.7/4.11.
62. Brace, L.H., W.T. Kasprzak, H.A. Taylor, R.F. Theis, C.T. Russell, A. Barnes, J.D. Mihalov and D.M. Hunten, 1987, "The Ion tail of Venus: Its Configuration and Evidence for Ion Escape," Journal of Geophysical Research, 92(A1), pp. 15-26.
63. Knudsen, W.C., A.J. Kliore and R.C. Whitten, 1987, "Solar Cycle Changes in the Ionization Sources of the Nightside of Venus," Journal of Geophysical Research, 92(A12), pp. 13391-13398.
64. Kliore, A.J., and R. Mullen, 1987, "Solar Cycle Influence on the Topside Plasma Scale Height of the Venus Dayside Ionosphere," Bulletin of the American Astronomical Society, 19, p. 846.
65. Lanzerotti, L.J., and C. Uberoi, 1989, "The Planets' Magnetic Environments," Sky and Telescope, 77(2), pp. 149-152.
66. Dickenson, R.E., and S.W. Bougher, 1986, "Venus Mesosphere and Thermosphere. I. Heat Budget and Thermal Structure," Journal of Geophysical Research, 91, pp. 70-80.
67. Bougher, S.W., R.E. Dickenson, E.C. Ridley, R.G. Roble, A.F. Nagy and T.E. Cravens, 1986, "Venus Mesosphere and Thermosphere. II. Global Circulation, Temperature and Density Variations," Icarus, 68, pp. 284-312.
68. A.E. Hedin, 1987, "MSIS-86 Thermosphere Model," Journal of Geophysical Research, 92, pp. 4649-4662.
69. Brace, L.H. and A.J. Kliore, 1990, "The Structure of the Venus Ionosphere," to be published in Space Science Reviews.

70. Brace, L.H., W.R. Hoegy, R.F. Theis, 1988, "Solar Euv Measurements at Venus Based on Photoelectron Emission from the Pioneer Venus Langmuir Probe," Journal of Geophysical Research, 93, p. 7282.
71. Hunten, D.M., 1982, "Thermal and Nonthermal Escape Mechanisms for Terrestrial Bodies," Planetary Space Science, 30(8), pp. 773-783.
72. Belotserkovskii, O.M., T.K. Breus, A.M. Krymskii, V.Y. Mitnitskii, A.F. Nagy, and T.I. Gombosi, 1987, "The Effect of the Hot Oxygen Corona on the Interaction of the Solar Wind with Venus," Geophysical Research Letters, 14, pp. 503-506.



Report Documentation Page

1. Report No. NASA TM-100761		2. Government Accession No.		3. Recipient's Catalog No.	
4. Title and Subtitle The Pioneer Venus Orbiter: 11 Years of Data A Laboratory for Atmospheres Seminar Talk				5. Report Date May 1990	
				6. Performing Organization Code 615	
7. Author(s) W. T. Kasprzak				8. Performing Organization Report No. 90B00109	
				10. Work Unit No.	
9. Performing Organization Name and Address Laboratory for Atmospheres Goddard Space Flight Center Greenbelt, MD 20771				11. Contract or Grant No.	
				13. Type of Report and Period Covered Technical Memorandum	
12. Sponsoring Agency Name and Address National Aeronautics and Space Administration Washington, D.C. 20546-0001				14. Sponsoring Agency Code	
				15. Supplementary Notes	
16. Abstract The Pioneer Venus Orbiter has been in operation since orbit insertion on December 4, 1978. For the past 11 years, it has been acquiring data on the salient features of the planet, its atmosphere, ionosphere, and interaction with the solar wind. <i>are summarized and discussed</i> The contents of this document are a summary of a few of the results of this mission and their contribution to our general understanding of the planet Venus. Although Earth and Venus are often called twin planets, they are only superficially similar. Possessing no obvious evidence of plate tectonics, lacking water and an intrinsic magnetic field, and having a hot, dense carbon dioxide atmosphere with sulfuric acid clouds makes Venus a unique object of study by the Orbiter's instruments. <i>is discussed</i>					
17. Key Words (Suggested by Author(s)) Venus Pioneer Venus Orbiter Venus atmosphere, ionosphere			18. Distribution Statement Unclassified - Unlimited Subject Category 88		
19. Security Classif. (of this report) Unclassified		20. Security Classif. (of this page) Unclassified		21. No. of pages 92	22. Price

National Aeronautics and
Space Administration

Washington, D.C.
20546

Official Business
Penalty for Private Use, \$300

Postage and Fees Paid
National Aeronautics and
Space Administration
NASA-451



NASA

POSTMASTER

If Undeliverable (Section 158
Postal Manual) Do Not Return
